

climate changes spatial planning

Climate scenarios

Refinement and application of a regional atmospheric model for climate scenario calculations of Western Europe

E. van Meijgaard | L.H. van Ulft | G. Lenderink | S.R. de Roode | L. Wipfler | R. Boers | R.M.A. Timmermans

KvR 054/12

Refinement and application of a regional atmospheric model for climate scenario calculations of Western Europe

Authors

E. van Meijgaard [1]
L.H van Ulft [1]
G. Lenderink [1]
S.R. de Roode [1]
L. Wipfler [2]
R. Boers [1]
R.M.A. Timmermans [3]

1 KNMI (Royal Netherlands Meteorological Institute), De Bilt
2 Soil Physics, Ecohydrology and Groundwater Management Group, Wageningen UR
3 TNO, Dept. of Climate, Air and Sustainability, Utrecht

Royal Netherlands
Meteorological Institute
Ministry of Infrastructure and the Environment

KvR report number KvR 054/12
ISBN ISBN/EAN 978-90-8815-046-3

This project (CS06; Refinement and application of a regional atmospheric model for climate scenario calculations of Western Europe) was carried out in the framework of the Dutch National Research Programme Climate *changes* Spatial Planning. This research programme is co-financed by the Ministry of Infrastructure and the Environment.

Contents

Summary

Summary in Dutch

Het KNMI regionaal klimaat model RACMO wordt in toenemende mate gebruikt bij de detaillering van Klimaatscenario's. Voorbeelden zijn de frequentie en intensiteit van hittegolven en de veranderingen daarin. Of te verwachten wijzigingen in het optreden van lokale neerslagextremen. In dit project zijn een aantal componenten van RACMO verder ontwikkeld. Het bestaande grenslaagschema is uitgebreid met een prognostische variabele voor turbulente kinetische energie waarmee de ontwikkeling van de grenslaag beter wordt beschreven. Deze aanpassing blijkt vooral de stabiele grenslaag beter te representeren. De bodemhydrologie van het model is verder verfijnd door ruimtelijke heterogeniteit in te voeren voor een aantal bodemparameters, zoals bodemtype en worteldiepte. Deze aanpassing resulteert in meer uitgesproken ruimtelijke structuren op regionale schaal. De nieuwe modelformulering is uitgebreid getest aan de hand van daggegevens van temperatuur en neerslag op Europese schaal. Verder is RACMO gekoppeld aan een regionaal chemie-transport model (LOTOS-EUROS) en is een module ingebouwd om het effect van aerosolen op wolken en straling te bepalen. Parallel aan de modelontwikkeling is de bestaande modelversie gebruikt in diverse toepassingen, waaronder het effect van een warme Noordzee op neerslag in de zomer boven land en de rol van temperatuur in extreme neerslagsommen op dag- en uurbasis. Een speciale toepassing betrof een bijdrage aan de Deltacie, waarin onder meer met RACMO gekeken is naar de verdeling van zwaarste stormen boven de Noordzee in het huidige en in een toekomstig klimaat.

Summary

The KNMI regional climate model RACMO is increasingly used in the refinement of climate scenarios. Examples include heat waves, in particular their frequency and intensity, the occurrence of local extremes in precipitation, and wind storms. In this project a number of components within RACMO have been further developed. The existing boundary-layer scheme has been extended with a prognostic variable for turbulent kinetic energy to improve the representation of a developing boundary layer. This modification turns out to be beneficial for the representation of the stable boundary layer. The soil hydrology component of the model is further refined by introducing spatial heterogeneity into a number of soil hydrology parameters, e.g. soil type and maximum root depth, which results in spatially more prominent structures at the regional scale. The new model formulation has been extensively tested at the European scale against daily observations of temperature and precipitation. In addition, RACMO has been coupled to the chemistry-transport model LOTOS-EUROS. A module has been incorporated in RACMO to account for the effect of aerosols to the cloud radiation interaction, the so called first aerosol indirect effect. Parallel to the model development, the existing model version has been used in various applications, e.g. quantification of the effect of anomalously high North Sea temperatures in summer to the intensity of precipitation over land and the role of temperature in the analysis of extreme precipitation at a daily and hourly scale. A special application regarded a contribution to the Delta Committee, which dealt with the distribution of heaviest storms over the North Sea as simulated by the model in the present-day climate and in a future climate.

Extended summary

Within the Climate Scenario theme (CS) of the Climate change Spatial Planning program (CcSP) the model refinement project CS6 had a central position. On the one hand it was meant to deliver direct model output produced by climate scenario calculations to project CS7, entitled "Tailoring climate information for impact assessment", where the material was further customized to meet the specific requirements of end users outside the CS theme or the CcSP program. On the other hand an important objective of CS6 was to improve the model formulation by further refining or developing representations of a number of physical processes that are considered relevant for an adequate simulation of present-day and future climate. To achieve this goal a strong collaboration was set up with several of the other projects within the CS-theme.

Together with project CS3, entitled "Soil moisture and root water uptake in climate models", causes to excessive soil drying in summertime, a problem that is frequently encountered in climate simulations, have been investigated in depth, resulting in potential solutions that were first implemented and tested in a SVAT (Soil Vegetation Atmosphere Transfer) scheme, which provides a very detailed representation of the relevant processes. From there the scope was upscaled by implementing the modifications into TESSEL (later HTESSEL), which is the land surface scheme of the regional climate model. Subsequently the revised scheme was tested and applied, first in a standalone version driven by external forcings, ultimately within the regional climate model environment interactively coupled to the other physics parameterizations and the dynamics.

Another development dealt with the representation of both the clear and cloudy boundary layer to include a prognostic variable for turbulent kinetic energy. Such approach is generally believed to yield a more physically sound representation of the evolving boundary layer compared to the customary first order K-diffusion description. Yet, it also adds a level of complexity in the numerical solution of the turbulent motions by the method of vertical diffusion coupled to organized cloud dry and moist convection in the lower troposphere. This development activity has been carried out within CS6.

A third model development issue concerned the aerosol effect on the climate. In collaboration with project CS4, entitled "Regional climate aspects of aerosols", a first step has been made in interactively coupling the regional climate model RACMO with the chemistry-transport model LOTOS-EUROS. This allows the quantification of the interactive effect of aerosols on the climate, and mutually the effect of weather and climate on air quality. The latter was achieved by adapting LOTOS-EUROS to be operated with atmospheric forcings from RACMO, while for the former a reversed coupler was built to interactively load RACMO with aerosol fields computed by LOTOS-EUROS. In addition to this, in close collaboration between CS4 and CS6, a conversion module was implemented in RACMO to express the LOTOS-EUROS inferred aerosol mass as number concentrations of cloud condensation nuclei and subsequently as cloud droplet effective radius which is the key microphysical parameter to estimate the effect of liquid water clouds on radiation. The representation in RACMO of two other important aerosol effects – the direct effect and the second aerosol indirect effect – are currently under development.

According to the proposals, other projects within the CS-theme with links to CS6 were project CS2, "The CESAR observatory: Climate monitoring and process studies", project CS8, "Time series analyses", and project CS5, "Remote influences on European Climate". From CS2 we used already existing cloud observations at Cabauw for the purpose of model evaluation at a single grid point. This approach was subsequently structured in a web page environment as a continuous long-term comparison of

single column output produced by various model versions with Cabauw measurements including observations of clouds, radiation and surface fluxes. It should be mentioned, though, that this type of comparisons is particularly suitable for testing parametric assumptions, rather than using it for direct model evaluation as it lacks spatial information across gradually changing climate regimes including underlying soils with highly different characteristics. Proposed links with CS8 have not been established because time frames between the projects did not match. In collaboration with CS5, we investigated the role of anomalously high North Sea temperatures to excessive amounts of precipitation that were recorded in August 2006 in the coastal zone of the Netherlands. With RACMO we examined the sensitivity of the precipitation events to changes in the prescribed North Sea surface temperatures. The primary finding from this study is that RACMO is capable of simulating the intensification in coastal precipitation triggered by high sea surface temperatures, however the model tends to release precipitation too close to the coastline. In our opinion, this shortcoming is a consequence of the use of parameterized convection. In another study, wind speed related output from a climate scenario calculation with RACMO at high resolution was compared with output from a number of GCMs obtained at much coarser resolution, and in addition with two re-analyses. This comparison indicated that, although high resolution is providing much more spatial refinement, it does in general not add information to the statistical distribution of high wind speeds associated to large-scale baroclinic instabilities that could not already be obtained from the coarser gridded models, as opposed to extreme precipitation. This is because the high wind speeds are associated to a large-scale phenomenon, whereas extreme precipitation events are frequently triggered by medium to small-scale atmospheric disturbances.

1. Introduction

Over the past couple of years there has grown a general recognition that regional climate models (RCMs) are potentially very helpful in adding quantified detail in future climate scenarios at the regional scale. Traditionally all information used in the formulation of climate scenarios is taken from the output of a few global climate models (GCMs), but the lack in resolution of the GCMs inhibits that model results are directly applicable at the scale of interest. Downscaling of GCM output with RCMs at high resolution may overcome this problem. In essence, the GCM provides the atmospheric circulation at the synoptic scale, while the RCM fills in the associated weather at a much finer scale. Added information is expected to be gained for parameters with fine spatial structures like precipitation, in particular extreme amounts of precipitation. Also for temperature added value is expected, especially for regions with a heterogeneous surface or in coastal areas. For a parameter like extreme wind speed the added value is expected to be small. This is because on the one hand the associated circulation is synoptic scale, i.e. at GCM-scale, while on the other hand the atmospheric structures favouring the most extreme wind speeds are generated at scales that are finer than current RCMs can resolve.

Project CS6 had two main objectives. 1) to produce a regional climate scenario calculation at unprecedented resolution both in space and time with means available at the start of the project, i.e. model, forcings, computing facilities (chapter 2). 2) to improve a number of known weaknesses in the model – the inability of the model to maintain very shallow boundary layers under stably stratified conditions, and the tendency of the model to overpredict temperature in summer in Central Europe (chapter 5) - and to introduce the representation of the first aerosol indirect effect (chapter

6), a process that was absent in the model so far. After a thorough evaluation with observations on temperature and precipitation, but also clouds and radiation, this part of the project should be finalized with defining an improved reference version of RACMO.

Besides these two main objectives the project intended to carry out and analyze a number of application studies (chapters 3 & 4). During the years of execution of the CcSP program insights in optimal application of RCM results for climate scenario construction developed strongly. While in late 2004 a large role of CS6 was envisaged to generate regional climate change scenarios used by CS7, these scenarios were developed from advanced interpretation of multi-model and observational data. Therefore, the need to apply and test a repeated climate scenario integration with the new RACMO upgrade was not considered of immediate relevance for the CcSP program. This activity is to be completed in the coming years in the context of other research programs (Kennis voor Klimaat; KNMI-next; CORDEX).

2. Climate Scenario Integration

2.1 Set up Integration

At the start of the project, the existing KNMI regional model RACMO, version 2.1 (van Meijgaard et al., 2008) was used to produce a multi-annual climate scenario integration (1950-2100) at high resolution (25 km, see left panel Fig. 2.1 for model domain) forced by information from a transient run with ECHAM5. The A1B SRES emission scenario was assumed (see right panel of Fig. 2.1). This activity was combined with work carried out in contribution to the EU-project ENSEMBLES (2005-2009).

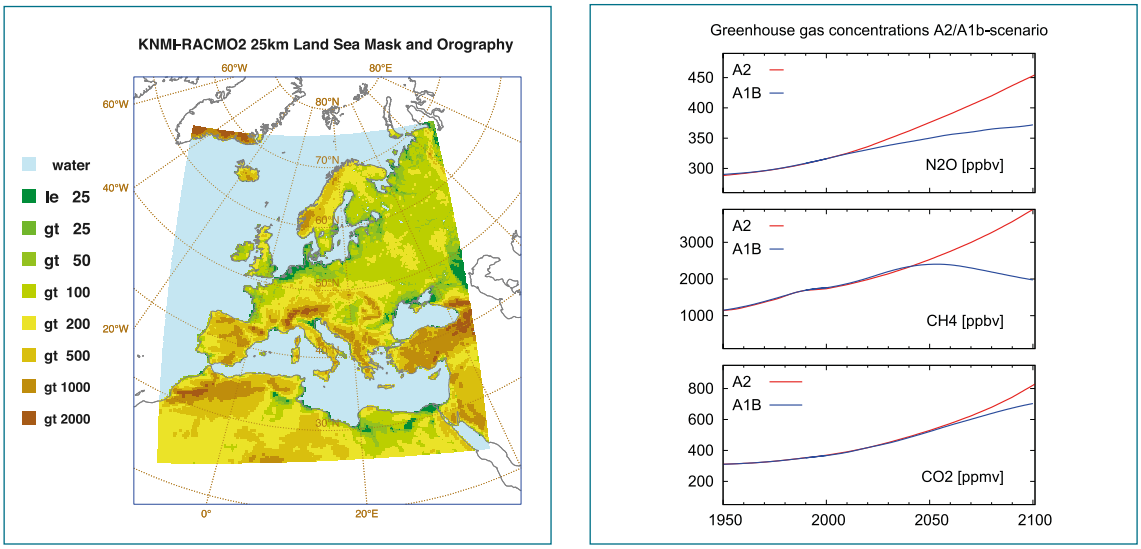

Figure 2.1.
RACMO2@25km orography and land sea mask (left panel) and time series of prescribed green house gas concentrations (both in ECHAM5 and RACMO2) under SRES A2 and A1B (right panel).

RACMO2.1 is primarily built on the dynamical core of HIRLAM6.3.7 and the physical parameterization package of the ECMWF model, cy23r4, but some components were taken from more recent releases (prognostic cloud scheme from cy25r4, cumulus convection scheme from cy28r1). Additionally, the physics package was adjusted by including a number of modifications, the details of which can be found in van Meijgaard et al. (2008). Direct model output from RACMO was postprocessed into the more convenient NetCDF file format suitable for users outside the modelling community.

2.2 Response of summertime temperature and precipitation

The response of model parameters to changing greenhouse gas concentrations is straightforwardly computed by comparing values between future climate and present-day climate. Time windows should be long enough, at least 30 years. Figure 2.2.a shows the response in summertime temperature and precipitation derived from the RACMO2 run forced with ECHAM5 fields obtained from a transient run. In this scenario mean summertime temperatures are expected to rise everywhere in Europe, but increases vary considerably from less than 1K rise in North Scotland to 6K in Central Spain. Also for summertime precipitation a strong north-south gradient is found with responses varying from 50% more precipitation in parts of Scandinavia to over 60% reduction in parts of the Mediterranean. However, overall amounts during summer are already very low in southern Europe giving to an unfavourably low signal to noise ratio as seen in the Figure.

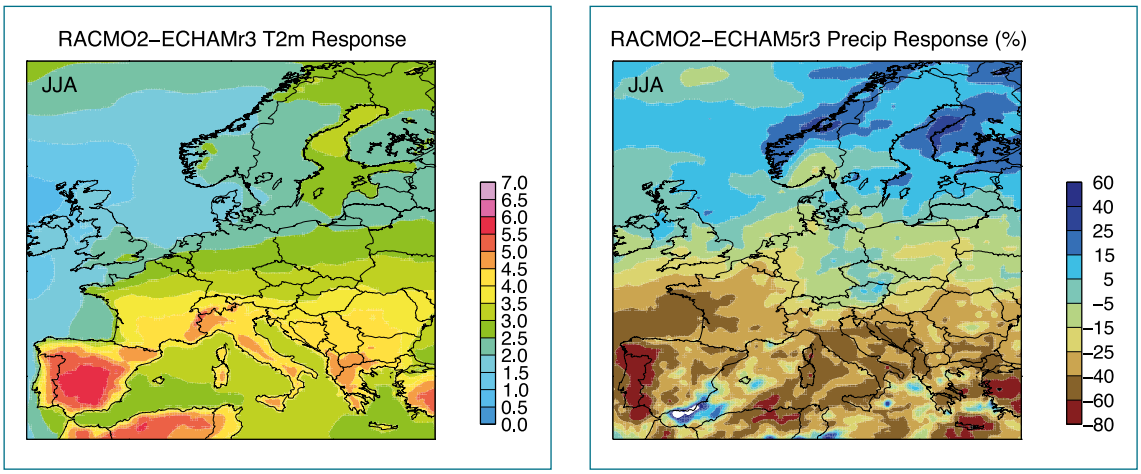

Figure 2.2.a.
Change in summertime 2m-temperature and precipitation derived from the 25 km RACMO2 climate scenario integration forced with fields from the ECHAM5 transient run, realization 3.

Clearly, one must regard Figure 2.2.a as the outcome of a scenario calculation and not as a prediction. Choosing a different RCM or GCM or emission scenario would result in a different response. Such issues have been systematically sorted out in previous EU-projects PRUDENCE and ENSEMBLES. The most important finding of these projects is that the spread in response between many RCMs all driven by the same GCM is much smaller than the spread of one RCM driven by different GCMs. The reason is that one given GCM provides just one realization with typical circulation statistics, which strongly constrains the spread of the RCMs when used as lateral forcing to the RCMs. But even then the variation between RCMs can be large, particularly in summer when large-scale synoptical forcings are less prominent.

To illustrate the role of the GCM, a second climate scenario integration was conducted forced with information from MIROC3.2 highres which exhibits a totally different climate change pattern than

ECHAM5. Results are plotted in Fig. 2.2.b showing different responses compared to Fig. 2.2.a. In particular the temperature response is much stronger with significant warming everywhere of at least 4K. Concerning precipitation the transition zone with zero change in precipitation is positioned much further to the south.

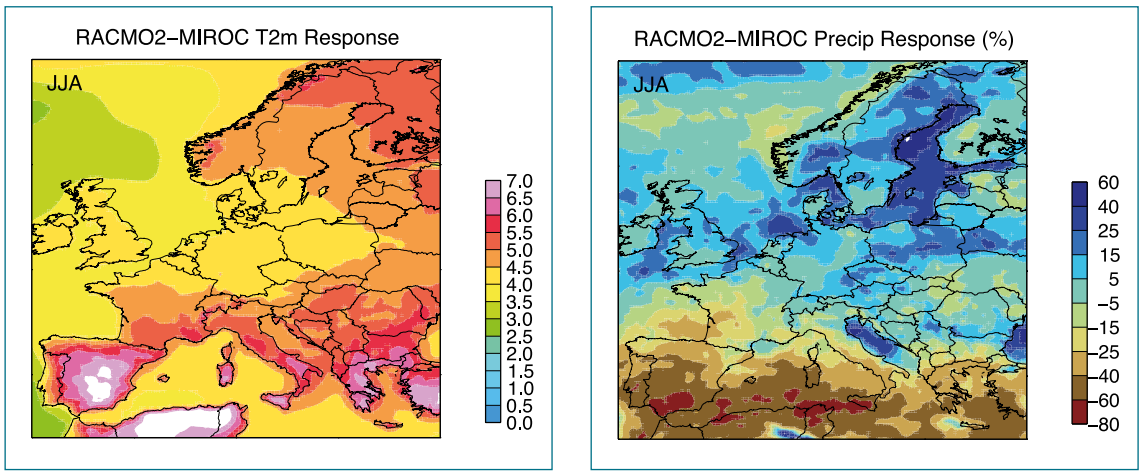

Figure 2.2.b.
Like Figure 2.2.a but with forcing boundary conditions adopted from MIROC3.2 highres.

2.3 Analysis of extreme precipitation

As pointed out in the introduction the added value of using RCMs is expected especially in the representation of extreme precipitation. In a recent paper Lenderink and van Meijgaard (2008) showed that observed scaling behaviour of extreme amounts of hourly precipitation with surface temperature is an increase of about 14%/K, which is twice as high as the increase op 7%/K that derived from arguments based on Clausius-Clapeyron. Although the reason for this enhanced scaling is not clear yet, an interesting result is that RACMO2 simulated extreme hourly amounts seem to scale likewise, in particular the highest percentiles (>99% of wet hours). This motivated us to compute the climate change signal of RACMO2 of extreme precipitation (Figure 2.3).

In large parts of Europe the rise in the 99.9th percentile of hourly precipitation is between 10 and 20% per degree temperature rise. Note that normalization is over all hours (days), while the scaling analysis is carried out over wet hours (days).

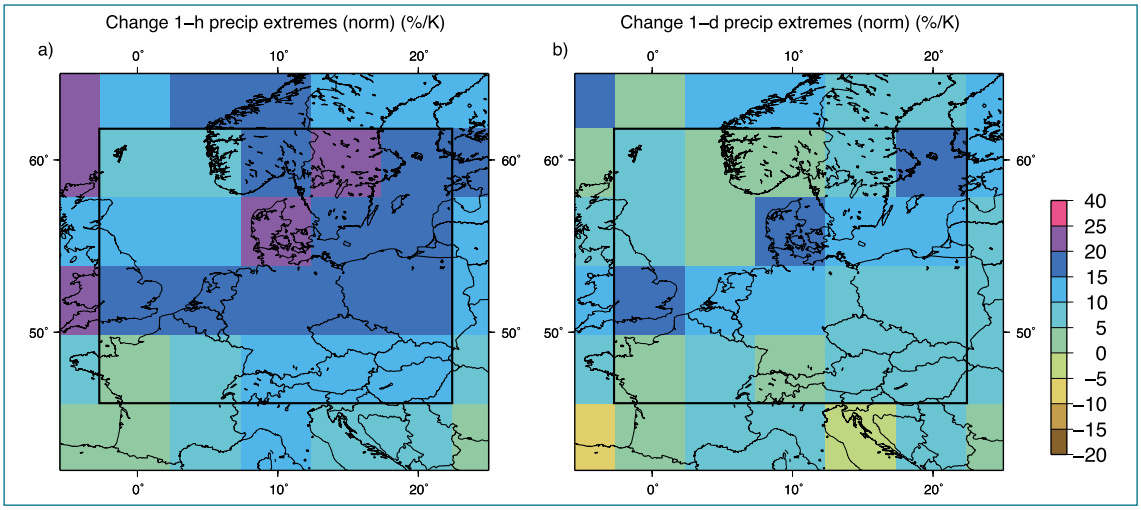

Figure 2.3.
The change in the 99.9th percentile of extreme precipitation on a grid scale (25x25 km) normalized by the seasonal mean local temperature change. Changes are computed from the difference between the future period 2071-2100 and the reference period 1971-2000. The check board pattern is the result of the statistical postprocessing in which data from a larger area is pooled together.

3. Impact of high North Sea temperatures on extreme coastal precipitation in summer

3.1 Introduction

August 2006 was characterized by extreme precipitation amounts in the Netherlands. Monthly precipitation sums locally exceeded 300 mm in the coastal zone; the average for the Netherlands was 150-200 mm, which is approximately 300 % of the climatological mean for August. Also on a daily level a large number of exceptionally high precipitation amounts were observed.

Extreme precipitation amounts reported in coastal areas in the Netherlands during August 2006 were primarily caused by a very persistent northwesterly flow of very unstable air resulting in an unusually high shower activity (see Figure 3.1). However, another factor was also believed to have induced the recorded high precipitation amounts. August 2006 was preceded by a record breaking warm July 2006, which at the end of July had resulted in very high sea surface temperatures (SST) of the North Sea, in particular in the coastal zones. These high sea surface temperatures led to a further destabilization of the atmosphere resulting in an increase of the already large – due to the unstable conditions – surface evaporation. This effect likely contributed significantly to the extreme precipitation in August.

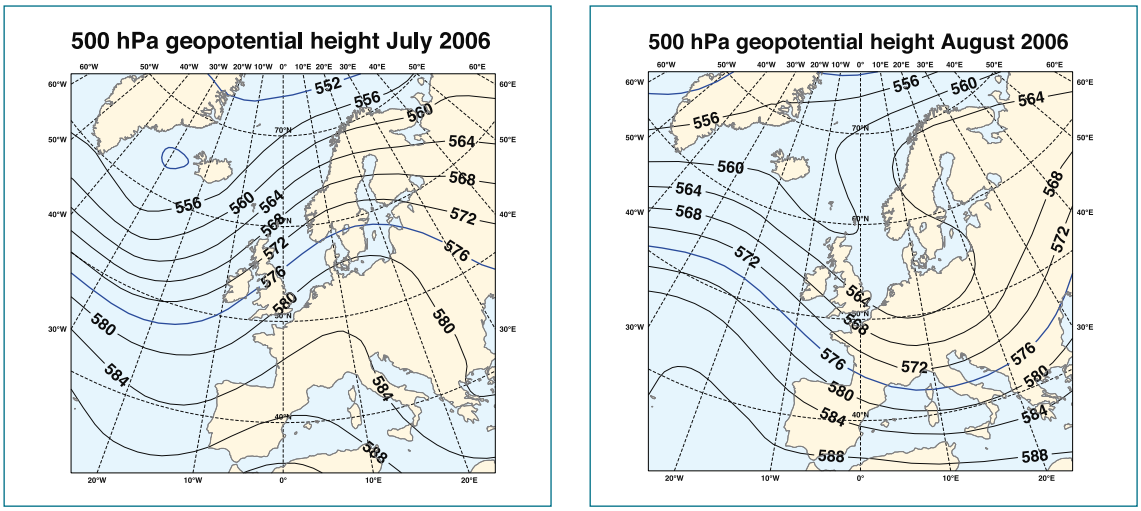

Figure 3.1.
Atmospheric circulation during July (left) and August 2006 (right). Shown is the 500 hPa height which reflects the atmospheric motions at a height of 5 km. Winds flow along the isolines from the west to the east. The blue line (576) roughly represents a division between the cold (and unstable) air to the north and warm air to the south.

3.2 Sensitivity runs with RACMO

We investigated this hypothesis by carrying out sensitivity runs with RACMO for distinctly different SST patterns while constraining each model integration with the same, observed, large-scale circulation. For this experiment the model domain was chosen approximately 1000 x 1000 km² and the horizontal grid spacing was taken 6km (Lenderink et al., 2009).

To analyze the influence of sea surface temperature (SST) in the North Sea on precipitation in the Netherlands a set of RACMO2.1 integrations with different SSTs was performed (Table 1). The reference run (denoted by NOAA) uses the "observed" SST field derived from NOAA satellite measurements during August 2006 (see Fig. 3.2.1a). "Observed" SST fields were obtained by aggregating satellite measurements at a nominal 1 km resolution to the model resolution of 6 km, which was found sufficient to resolve the coastal waters, including the Wadden Sea, lake Yssel, and the larger bodies of the Zeeland waters. Weekly composites of SST patterns were compiled to retain enough cloud free images per pixel. In addition, we performed four runs with different 10-year climatologies (denoted by CLyy, with yy the 10-year period), all having lower SSTs than was observed in the summer of 2006. The 1981-1990 mean SST is shown in Fig. 3.2.1b. These SST climatologies are based on the ERA40 re-analysis (www.ecmwf.int/research/era/) and lack the sharp gradients near the coast. Part of this gradient may be caused by the warm July month. However, due to the lack of a sufficiently long observational data set of SST it is not possible to verify this statement. We therefore supplemented the CL runs with one run (NOAAM2) in which the gradient near the coast is retained by subtracting 2° C from the NOAA observed SST.

Table 3.2.
Overview of the experiments with RACMO2

Experiment	Derived from
NOAA	Observed SST derived from NOAA measurements
NOAAM2	OBS, but with 2 °C subtracted
CLyy	ERA40 derived SST, with yy referring to a 10-year averaging period

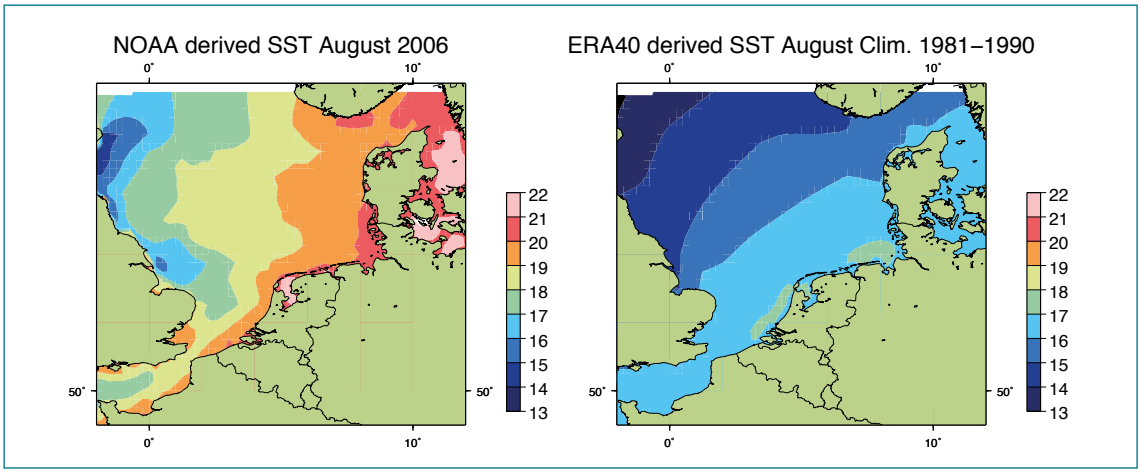

Figure 3.2.1.
Observed SSTs inferred from NOAA satellite measurements for August 2006, and ERA40 derived climatological SST for the period 1981-1990.

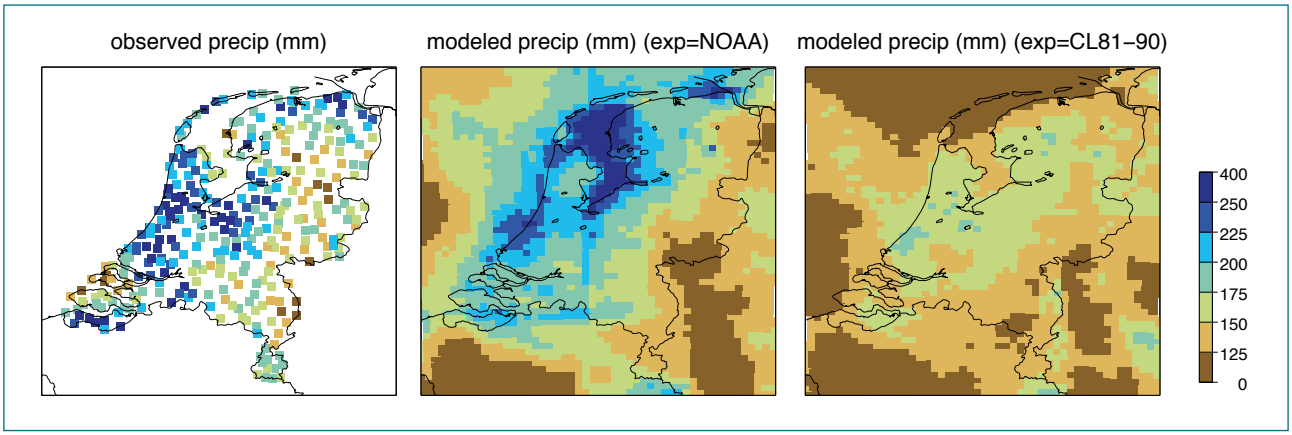

Figure 3.2.2(a).
Observed precipitation amount (left), and modeled precipitation amount in experiments using observed SST (NOAA) (b, middle), and a "cold" SST (CL81-90) (c, right panel) in August 2006 (mm).

The observed precipitation sum in August 2006 is shown in 3.2.2. Near the coast and lake Yssel (big lake in Northwestern part of the Netherlands) the average precipitation sum is 210 mm, with maxima of near 300 mm at a few locations. Inland precipitation amounts are 150-180 mm on average. The climatological average (1971-2000) for August is 62 mm in the coastal areas and 60 mm inland.

The simulated precipitation amounts for the experiments NOAA and CL81-90 are also shown in 3.2.2. In the run with observed SST (NOAA) the regional model reproduces the high precipitation amounts

in the coastal zones, and the lower amounts further inland. Despite the general correspondence, the maxima in precipitation do not always agree well with the observations, in particular near the lake Yssel where the model appears to produce unrealistically high precipitation amounts. Inspection of accumulated rainfall inferred from rain radar measurements did not show signs of the high amounts over the lake Yssel. The sensitivity experiment using the ERA40 derived SST 1981-1990 climatology (CL81-90) does not show the intensification of rainfall in the coastal areas. The amounts further inland, however, are comparable to the reference experiment (NOAA). Results of the other sensitivity experiments are similar to CL81-90 with (very) weak coastal intensification of the rainfall.

To further quantify the coastal effects, we analyzed rainfall as a function of distance to the coastline. For this purpose, we divided the Netherlands in different regions (zones) based on the distance to the coastline (the coastline includes lake Yssel). Sea surface temperatures and rainfall amounts are plotted in 3.2.3 as averages of the different zones. SST gradients near the coast in the CL runs are small due to the coarse resolution of the underlying ERA40 data. There is a significant trend in time with the 1991-2000 period being approximately 1.5˚C warmer than the 1961-1970 period. Precipitation amounts over land in the NOAA experiment follow the observed precipitation rather closely, but there is a spatial shift of approximately 20 km (shifted to the sea). All sensitivity experiments show lower precipitation amounts in the coastal zone by 30-60 mm month^{-1}. Further inland, the differences with NOAA are less than 20 mm month-1. Further analysis indicated that most of the sensitivity to the SST was concentrated in the first half of the month. We also note that the initially very warm sea water near the coast rapidly cooled down in the course of the month.

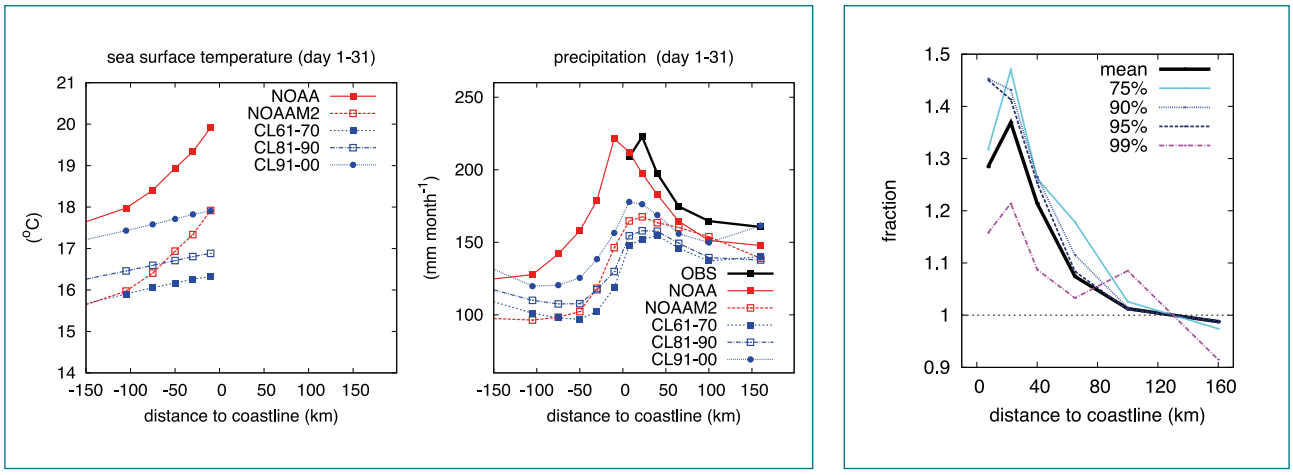

Figure 3.2.3.
Sea surface temperature (left panel), and precipitation (central panel) as a function of distance to the coastline (black line: observed precipitation derived from 324 stations). Right panel shows the observed mean and extreme precipitation amounts in August as a function of distance to the coast. Shown are relative differences (fraction) with the inland values (inland values are defined as the average value at 100 and 160 km). Statistics are based on the pooled station data of the different zones.

The observed intensification of rainfall in the coastal area compared to the inland area is shown in the right panel of Fig.3.2.3 for both the mean and the extreme precipitation amounts. Extreme precipitation amounts are computed from the pooled data of the stations in different zones, and therefore represent local extremes on a station level. Except for the most extreme 99-percentile, local rainfall amounts in the coastal zone are approximately 30-40% higher than the inland values. For the most extreme events represented by the 99-percentiles the coastal intensification is smaller, between 10 and 20 %. Partly, this may be due to statistical uncertainty. With on average 30-50

stations in a zone, the 99-percentile reflects only 9-15 events. Yet, it may also be explained by a longer lifetime of the strongest and largest shower complexes, which enables a further penetration inland. Concluding, not only the mean precipitation shows the coastal intensification, but also extremes are stronger in the coastal zone.

4 High wind speeds

4.1 Case study of 1953-storm with varying horizontal resolution and varying forecast time

Concerning the occurrence of high wind speeds associated to large-scale baroclinic instabilities one might wonder whether high resolution models provide added value in representing this type of events. To investigate this issue we devoted a brief case study to the event of the 1953 storm to examine the sensitivity to horizontal resolution and forecast time. Although outside the ERA-40 time window and prior to the International Geophysical Year in 1957 ECMWF has reconstructed the large-scale features of this storm, commonly referred to as the Dutch storm, in great detail on the basis of a special observational dataset compiled by NCEP (Jung et al., 2003), at the occasion of the 50-year commemoration of this event. The corresponding set of reanalyses, covering the period 20 January until 6 February 1953, served as lateral boundary conditions in our case study.

First we examined the sensitivity of the model predicted mean sea level pressure and 10-meter wind speed to the horizontal resolution as displayed in Figure 4.1.1. Shown are the ECMWF analysis verifying at 00 UTC on 1 February 1953 along with results from five 36-hour hindcasts at different horizontal resolutions all initialized at 12 UTC on 30 January 1953: LCB54: large domain with 54 km mesh; KVR25: large domain with 25 km mesh; KVR12: large domain with 12 km mesh; MCB18: medium-sized domain with 18 km mesh; HCB06: small domain with 6 km mesh. The LCB54/KVR25/KVR12 are forced from ECMWF-analysis, while MCB18 is nested in the LCB54 result and HCB06 is nested in the MCB18 result.

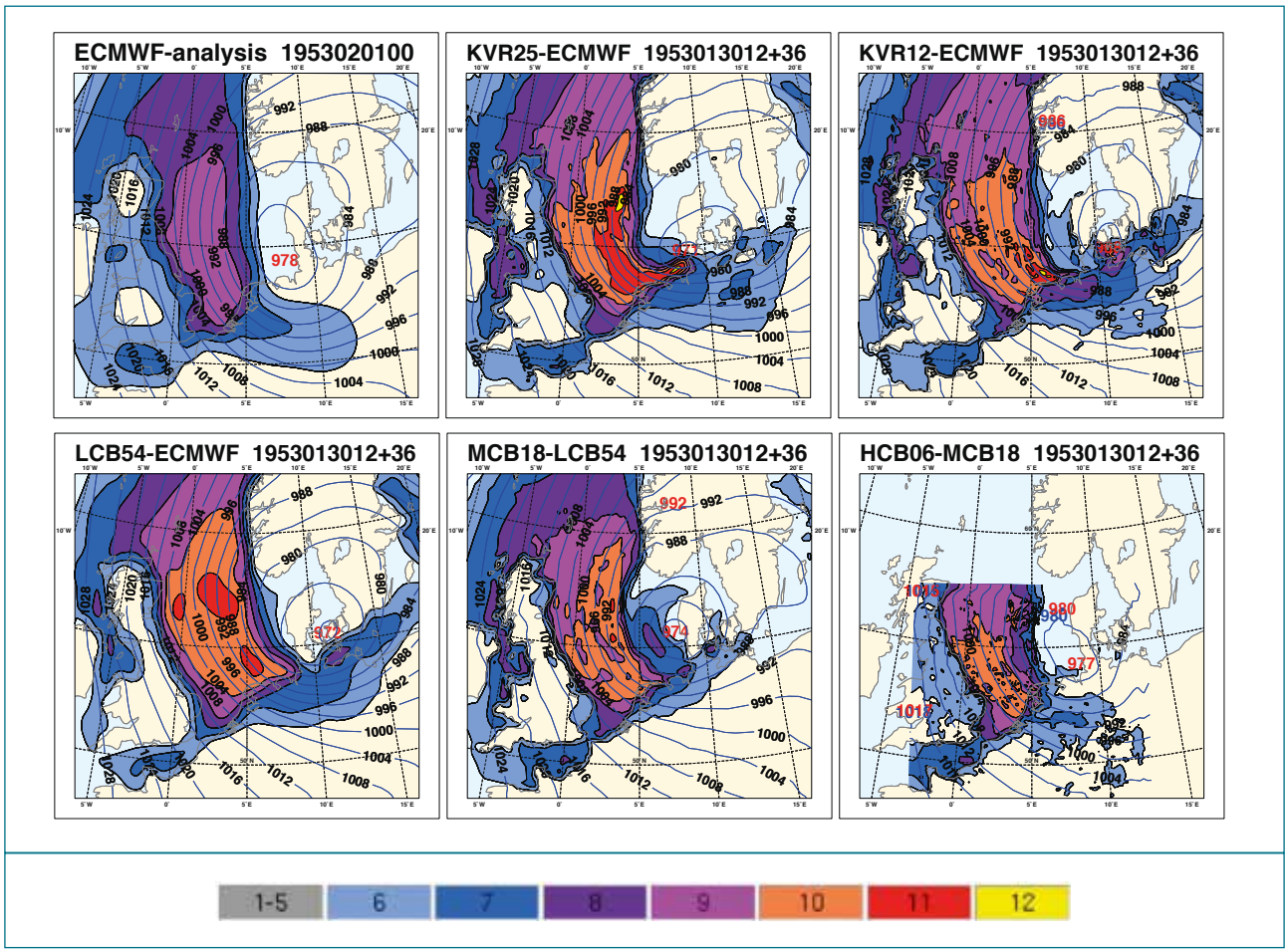

Figure 4.1.1.
ECMWF analysis (upper left panel) and 36-hour RACMO predictions at various domain sizes, resolutions and forcing strategies of mean sea level pressure and instantaneous 10-meter wind speed all verifying at 00 UTC on 1 February 1953. Colors label the strength according to the Beaufort-scale.

Several features are worth pointing out. The RACMO predicted wind field is much stronger than indicated by the analysis. While the ECMWF analyzed wind speed does not exceed 9 Bft, the model predicted wind speeds are 10 Bft over a considerable part of the North Sea with sizeable areas of 11 Bft and patches of 12 Bft. There are several factors that contribute to this difference. Firstly, the re-analysis is obtained at a coarser resolution than used in RACMO. Secondly RACMO employs a modified Charnock relation yielding higher wind speeds in the high wind speed regime. Thirdly, the west-east pressure gradient across the North Sea at 55oN is somewhat stronger in RACMO than in the analysis. Also the predicted maximum wind speed field is shifted to the east relative to the verifying analysis, which seems consistent with the finding that the centre of low pressure in all RACMO hindcasts is predicted east to the analyzed position, while the predicted position of the 1020 hPa isobar is also shifted somewhat to the east. Also the predicted central pressure is 4 to 6 hPa below the analyzed value, which is a robust feature found in all RACMO predictions. According to historical surface maps the minimum surface pressure was slightly below 976 hPa. Varying horizontal resolution has relatively little impact, with the exception of details in the wind speed field in the vicinity of land-sea transitions. This is clearly illustrated by the three figures in the bottom row of Figure 4.1.1, which are remarkably similar in location and depth of the low pressure system and in extent and intensity of the wind field. These runs differ only in horizontal resolution, as application of multiple one-way nesting leads these integrations to be driven by essentially equivalent forcings.

Another sensitivity that we have examined is the lead or forecast time (or better phrased hindcast time as lateral forcings are provided by (re-)analyses rather than forecasts) in order to see whether the accuracy in predicting the position and depth of the low pressure system at verifying time can be improved. For this we have carried out a number 25 km runs, each member with a different initial time varying from 84 hours until 6 hours prior to verifying time.

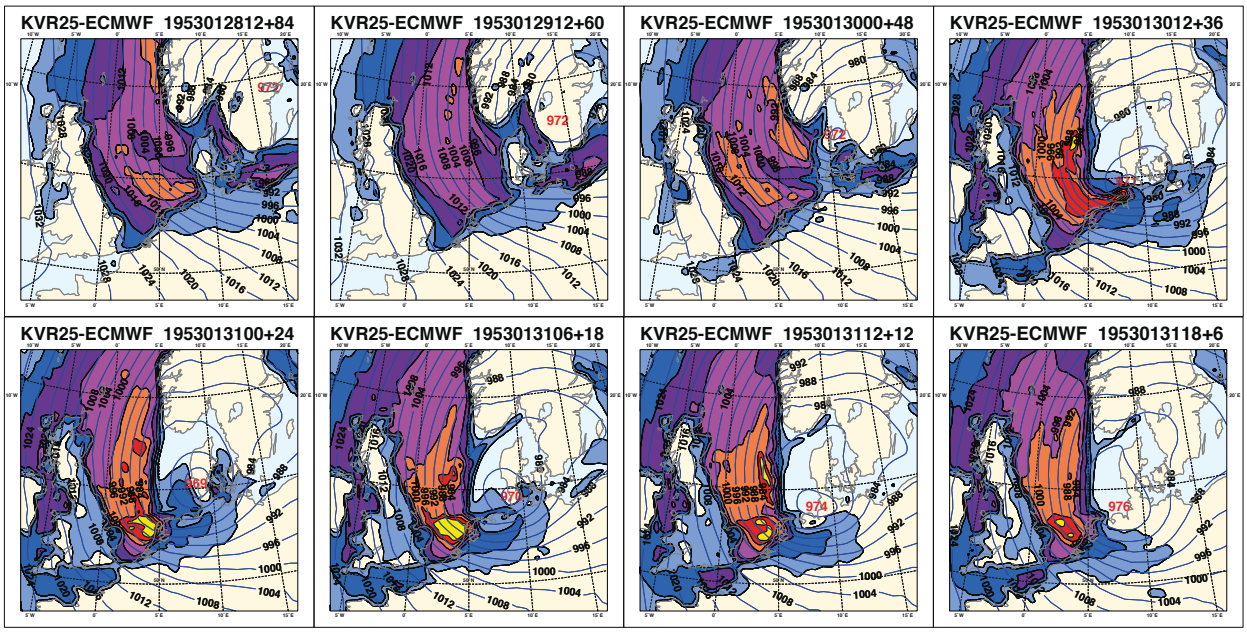

Figure 4.1.2.
RACMO predictions at 25 km resolution (domain KVR25) with different forecast or lead times verifying at 00 UTC on 1 February 1953. Lead times from left to right in top row: 84, 60, 36, 24 hours; bottom row: 24, 18, 12, 6 hours. See Figure 4.1.1 for meaning of colors.

The eight forecasts shown in Figure 4.1.2 share the common feature of a storm field over the North Sea at verifying time, however details are very different. For lead times of 36 hours or more the position of the low pressure system is way off to the east resulting in too low wind speeds. A comparable result was found in examining the skill of medium-range forecasts with the ECMWF model (Jung et al., 2003). For shorter lead times the prediction of the low pressure system position gradually improves but the predicted depth of the system remains too low – even 969 hPa for the t+24 forecast – which results in too intense wind fields. The hindcast with the shortest lead time of 6 hours seems best performing in terms of position and depth of the low pressure system and position of the wind field, however obviously a forecast with such short lead time might in practice be considered now-casting, which is from a forecasting perspective not very useful. Yet, it is encouraging to see that there exists a selection of run-time parameters in which RACMO provides a skillful performance. At the same time we may conclude that in a climate-type integration – in the context of the above an integration with “infinite” forecast (hindcast) time – it is unlikely that RACMO or RCMs in general when forced from (re-)analyses, i.e. observed atmospheric states, are capable of accurately capturing the details of a large-scale storm event. Either the position of the low pressure system is not optimally reproduced, or its intensity, or both. So, the general features of large-scale storm events will be captured, but not accurately in its detail. A side conclusion is that horizontal resolution is not a critical parameter, provided it is finer than a threshold resolution in the order of 50 km.

4.2 Contribution to the Delta Commitee

Half-way CS6 KNMI was requested by the Delta Committee, installed by the Dutch Government, to make a science based estimate concerning the potential impact a changing climate might have on the expected 10000-year return water level. To address this issue KNMI carried out a study based on a 17-member ensemble of North-Sea water levels spanning the period 1950-2100. All members were obtained by forcing the surge model WAQUA with meteorological information from transient runs conducted in the ESSENCE project with the ECHAM5 GCM under the assumption of the SRES A1b scenario. The main outcome of the study is that from the multiple simulations with this GCM no statistically significant change in the 10000 year return values of surge height along the Dutch coast during the 21st century is found (Sterl et al., 2009). As a transient run with RACMO driven by identical forcings was already available at much higher resolution – 25 km – compared to the ESSENCE members – about 200 km – the results of this run were used to examine whether the resolution of meteorological data had an effect on the offset and direction of the return level of daily-mean wind speed expressed in terms of a Gumbel variate, as shown in Figure 4.2.

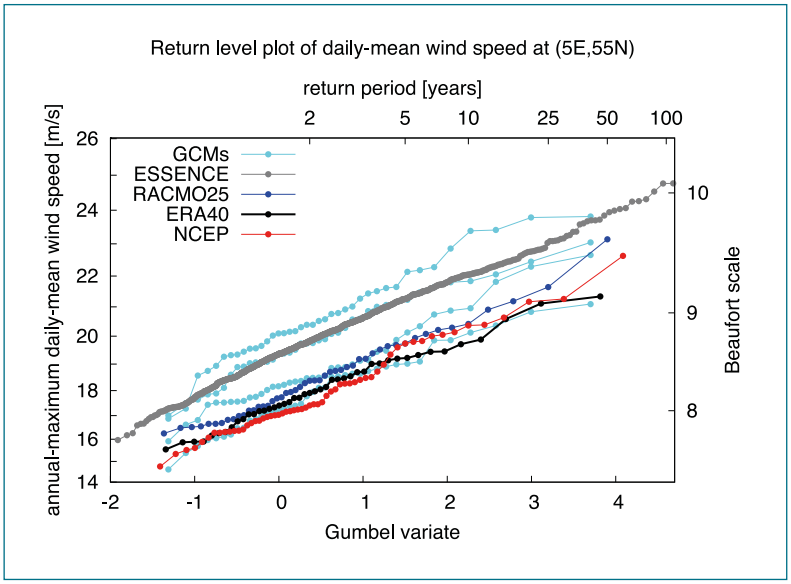

Figure 4.2.
Gumbel plot of annual-maximum daily-mean wind speed at 5E, 55N.The Gumbel variate (lower horizontal axis) is a transformed rank variable, which is directly related to the return time (upper horizontal axis), i.e. the average time between two occurrences of a given value. The grey line indicates the result from the ESSENCE ensemble (17 members pooled in one data set), the red and black line represent the result for the reanalyses from NCEP and ERA-40, respectively, while the blue line denotes the result from a 25-km transient run with RACMO. The cyan lines denote the result from various other GCMs.

No effect on the direction is found, while the effect on offset is likely more the result of using a different parameterization to relate wind speed to roughness length than what is used in ECHAM5 than that it is caused by finer resolution. Concerning the contribution of RACMO, a plausible conclusion drawn from this work is that RACMO – and probably regional climate models in general – do not provide much added value in representing synoptic-scale low pressure system induced high wind speeds. What we might expect though is a finer resolved spatial structure, which may be beneficial, in particular in coastal areas.

5. Model Development and Evaluation

5.1 Introduction

Model development in CS6 partly focused on improving known model deficiencies. A general problem that is seen in RACMO but also in many other models is the inability to maintain very shallow stable boundary layers. As a result, in regions with persistent stable conditions depending on the season like e.g. Northern Scandinavia in winter model simulated near surface temperatures are on average far too high, up to 10K. One way to improve the situation is to replace the first order closure by a turbulent kinetic energy closure which produces less mixing and hence might allow the evolution of shallower boundary layers.

Another known deficiency, also seen in many other models, is the tendency to considerably overestimate near surface temperatures in Central Europe in summer. This problem was already noticed in a very early version of RACMO2 and then partly solved in an ad hoc way by modifying soil hydrology parameters. In collaboration with project CS3 an effort has been made in resolving this issue by taking a more physics oriented approach.

5.2 New baseline reference

All model developments in CS6 have been implemented in a new baseline reference version which was built on the ECMWF model cycle 31 release 1. Eventually, the newly built RACMO version will be referred to as RACMO2.2. Version 2.1 is built on cy23r4 which formed also the basis for the ECMWF Re-Analysis system ERA-40. Likewise cy31r2 (which is very close to cy31r1) forms the basis of the reanalysis ERA-Interim (Dee et al., 2011). Moreover, cy31r1 was the starting point for the EC-Earth global climate model project which is co-coordinated by KNMI (Hazeleger et al., 2010). Along with the new baseline came a number of changes, some of them with a potentially major impact. Most noteworthy is the introduction of the externalized surface scheme (in cycle 29) which implies a radical change of the model code structure. Other major modifications include an upgraded deep convection scheme, the introduction of an eddy-diffusivity mass flux scheme to solve simultaneously for turbulent mixing and convection in the boundary layer, the introduction of form drag to describe in the interaction of the near surface flow with sub-grid scale orography, a corresponding reformulation of the roughness length, a new aerosol climatology, and a new prescription of effective cloud droplet radius and cloud crystal size.

5.3 Boundary layer mixing scheme

A new unified boundary layer mixing scheme has been developed and implemented in RACMO2.2. This scheme is based on two schemes that were developed earlier: i) a moist TKE scheme and ii) a dual mass flux scheme (Siebesma et al., 2007; Neggers et al. 2009; Neggers, 2009). The moist TKE scheme is based on an equation for turbulent kinetic energy (TKE) and includes moist cloud physics. It was designed for stably stratified atmospheric boundary layers (Baas et al. 2008), and cloud topped boundary layers with 100 % cloud cover (Stratocumulus). The dual mass flux scheme is based on two updrafts that represent non-local transport in dry convective and cloudy boundary layers due to the strongest vertical motions. The dual mass flux was specifically designed for unstable boundary layers, and cloudy boundary layers with broken clouds (Cumulus). As part of CS6 these two schemes have been merged to obtain one unified scheme representing mixing in stable,

dry convective, and cloud-topped boundary layers with both broken (Cumulus) and solid cloud decks (Stratus/Stratocumulus). Since both schemes turned out to interact quite strongly, merging them was far from trivial. The mass flux scheme had to be simplified, while retaining its main properties. Also the TKE scheme had to be adapted in order to be able to work together with the mass flux scheme.

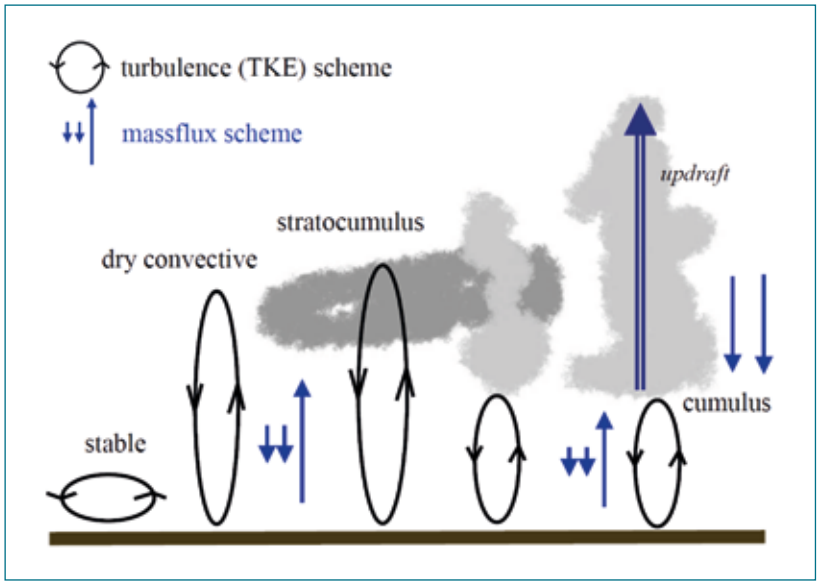

Figure 5.3.
Schematic overview of the unified scheme and different boundary layers and clouds. Blue arrows are indicating mixing by the mass flux scheme, where black ovals are indicating mixing from the TKE scheme.

The performance of the new boundary layer scheme is discussed in paragraph 5.6 “Evaluation of Temperature and Precipitation”.

5.4 Soil Hydrology

As mentioned before many models including the ECMWF model and hence also RACMO (as it employs the ECMWF physics package) show a tendency of soil drying in summertime and in response too dry and too warm near surface atmospheric conditions. In the ECMWF model this tendency is counteracted by a positive soil moisture supply to the model state through the data assimilation system. In a climate model, this correction mechanism can not be applied and one needs to improve the parameterization. In an earlier version of RACMO an ad hoc remedy was installed by deepening the soil layers, hence allowing for enhanced buffering of winter precipitation, and modifying the formulation of evaporation of vegetated surfaces to available soil moisture. The effect on summertime temperatures is shown in Figure 5.4.

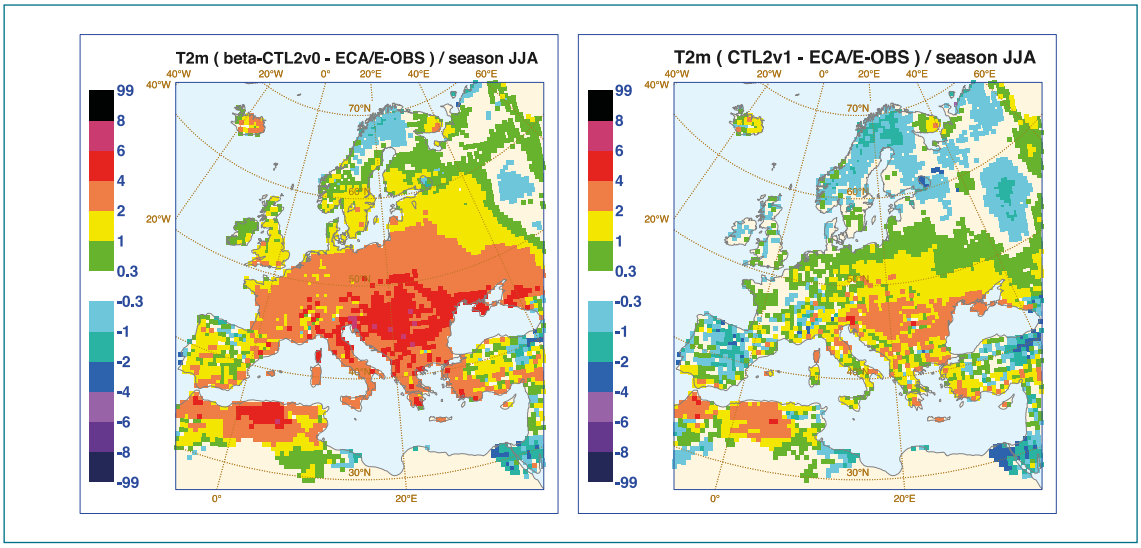

Figure 5.4.
Bias in 2-meter temperatures during summer (JJA) for an integration excluding (left panel) and including (right panel) changes in soil depth and water stress (see text for explanation).

In collaboration with CS3 (Wipfler at al. 2011) an effort has been made to establish a more physics oriented approach of the ad hoc alterations in the soil hydrology component, and also to introduce spatial heterogeneity in soil hydrology parameters. The first step consisted of replacing the land surface soil scheme TESSEL by its successor HTESSEL (made operational in cy32r3). An important new feature in HTESSEL (Balsamo et al. 2009) is the use of a soil texture class which is used to specify the soil hydrology parameters. The use of classes already introduces spatial heterogeneity which was absent in TESSEL. Other new features in HTESSEL, all of them only affecting the soil hydrology, include modified hydraulic properties for unsaturated soils, and a new surface runoff scheme based on sub-grid scale orographic variance. The new hydrology scheme yields a displaced soil moisture equilibrium and an increased response in surface runoff, however surface evaporation is hardly affected.

Within CS3 two issues have been addressed that relate to the ad hoc changes implemented in an earlier version. Firstly, water stress on the canopy resistance has been formulated in terms of water pressure difference rather than in terms of soil moisture. Instead of the linear water stress reduction formula this results in strongly non-linear curve which is nearly constant for soil moisture values in a considerable range below field capacity, and only when soil moisture comes in the vicinity of the wilting point the reduction grows very steeply. In this approach soil moisture from the canopy is available for evaporation without stress for a large range of soil moisture values, in contrast to the original formulation. In general, this modification leads to a more intense hydrological cycle, and considerably lowers near surface temperatures. Secondly, the issue of soil depth was addressed, however with the somewhat unexpected outcome that the default total soil depth of 2.89 meter in HTESSEL was considered too deep for many of the land grid points as opposed to what was essentially assumed in the ad hoc modification. The rationale that led to the new insight is that the effective soil depth for water storage is often limited by rocks or rocky material in the soil. Because the method of solution of the heat equation in the soil assumes a zero flux at the bottom of the column and can therefore not be applied to shallow columns, we modified the parameter representing maximum rooting depth instead of soil depth. Four more depth classes have been introduced, i.e. 10, 60, 80, 100 cm, in addition to the default soil depth. The effect of this modification is suppression of the hydrological cycle, resulting in higher near surface temperatures than the reference. However, this applies only to those grid points which do not fall in the default class.

5.5 Leaf Area Index

In the (H)TESSEL surface scheme the Leaf Area Index (LAI, m^2 leaf / m^2 ground) is defined per vegetation type from which it derives its spatial variation. However, the prescribed LAI-field is constant throughout the year with above average values in winter and spring and below average values in the other season. This may lead to substantial overestimation of evapo-transpiration in spring when the vegetation is still developing, resulting in too dry soils once the summer starts. To improve the situation we introduced intra-annually varying LAI maps. In collaboration with CS3 and WaterWatch we derived LAI maps per ten-day period for Europe (11°W – 62°E; 25°N – 75°N) from SPOT vegetation satellite images averaged over 1999 to 2005, using a method described in Knyazikhin et al. (1999). For a RACMO simulation the high-resolution LAI values are linked to vegetation type and averaged over the grid box to obtain LAI values for low and high vegetation. Figure 5.5 illustrates the variation in the LAI derived from SPOT in space and time.

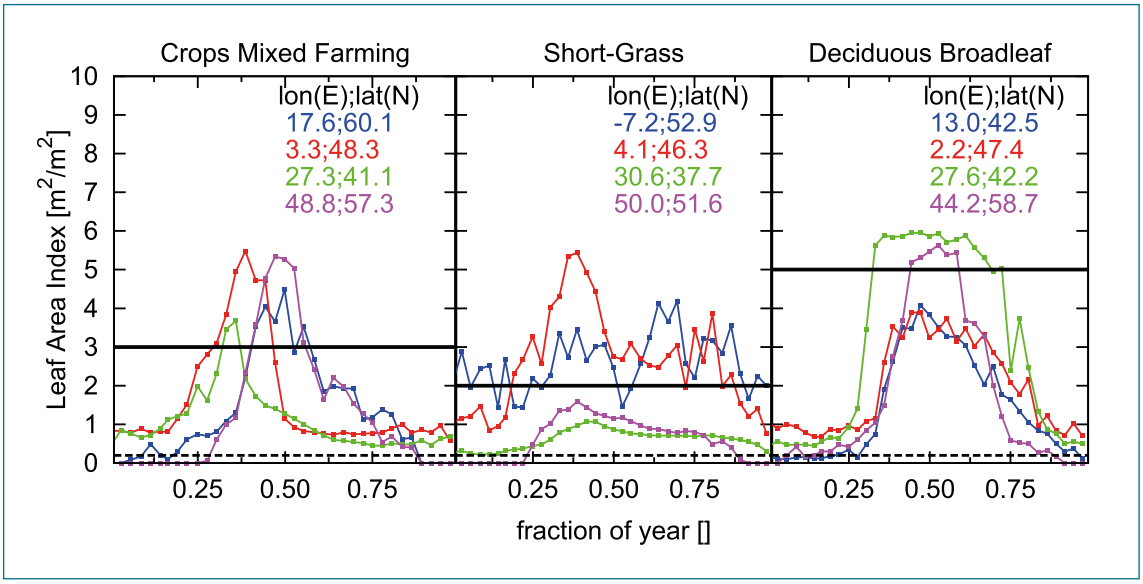

Figure 5.5.
Seasonal Cycle in Leaf Area Index for various vegetation types and various locations across Europe (four solid colored curves). The solid black curve indicates the vegetation-dependent annually constant LAI-value used in the original model formulation. The dashed black curve designates the threshold value imposed to LAI in the new formulation.

5.6 Evaluation of Temperature and Precipitation

In order to assess the performance of the various model versions we have carried out an evaluation against ECA/E-OBS version 2 daily high resolution gridded data on temperature and precipitation compiled within EU-ENSEMBLES (Haylock et al., 2008; http://eca.knmi.nl). For this purpose model versions were integrated over the 8-year period 2000-2007 at 50 km resolution, all forced by ERA-Interim fields at lateral boundaries and sea surface boundaries. Model versions that were considered are listed in table 5.6:

Table 5.6.
Description of Model Experiments.

Number	Acronym	Description
EXP00	ECA/E-OBS	Observations
EXP01	CTL2v1	Control version RACMO2.1
EXP02	STD-CY31	Baseline version with physics from ECMWF Cycle31r1
EXP03	STD-CY31-vdfexcu-CY32r3	Built on STD-CY31 with reduced mixing in free troposphere adopted from CY32r3
EXP04	dualM-TKE	TKE scheme built on STD-CY31
EXP05	CS6-HTESSEL-LAI-TKE	Built on STD-CY31, including HTESSEL, LAI and TKE
EXP06	CS3-trlh-CS6-LAI-TKE	Built on CS6-HTESSEL-LAI-TKE + reformulated water stress
EXP07	CS3-rtdec-CS6-LAI-TKE	Built on CS6-HTESSEL-LAI-TKE + varying maximum root depth
EXP08	CS3-trlh-rtdec-CS6-LAI-TKE	Combining EXP06 and EXP07
EXP09	ERAIN: i.e. ERA Interim reanalysis (NOT a RACMO-run)	Temperature: t+00 Precipitation: t+00 --- t+12
EXP10		Precipitation: t+12 --- t+24

Evaluation of daily mean 2-meter temperature

The bias in mean wintertime temperatures (DJF) of EXP02 and EXP04 are shown in Figure 5.6.1. The spatial pattern found for EXP02 is typical for all runs: a strong gradient in bias from positive in Northern Europe (with the exception of the Norwegian mountains) to negative in the Mediterranean. A beneficial outcome of implementing the TKE closure in the boundary-layer scheme is that it indeed considerably reduces the bias in North Scandinavia where stable conditions in winter tend to be persistent.

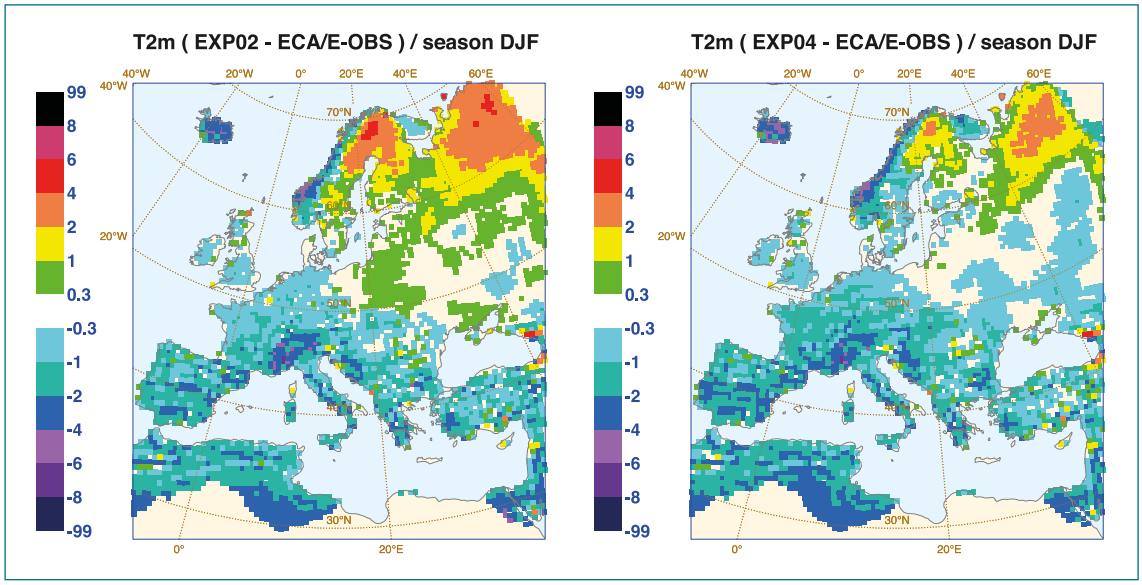

Figure 5.6.1.
Bias in mean winter temperature for the baseline version (EXP02) and a version including TKE (EXP04).

Likewise, the bias in mean summertime temperatures (JJA) of EXP02 and EXP05 are shown in Figure 5.6.2. The bias plot for EXP02 shows a typical structure with extensive positive biases in Central Europe up to the Black Sea, and also in the Western part of North Africa. Negative biases are scattered in the periphery of the European continent. The reduction in positive bias seen in EXP05 is primarily due to substituting HTESSEL for TESSEL, and to some extent to TKE. The role of seasonal varying leaf area index (LAI) is beneficial but more so in winter and spring than in the other seasons.

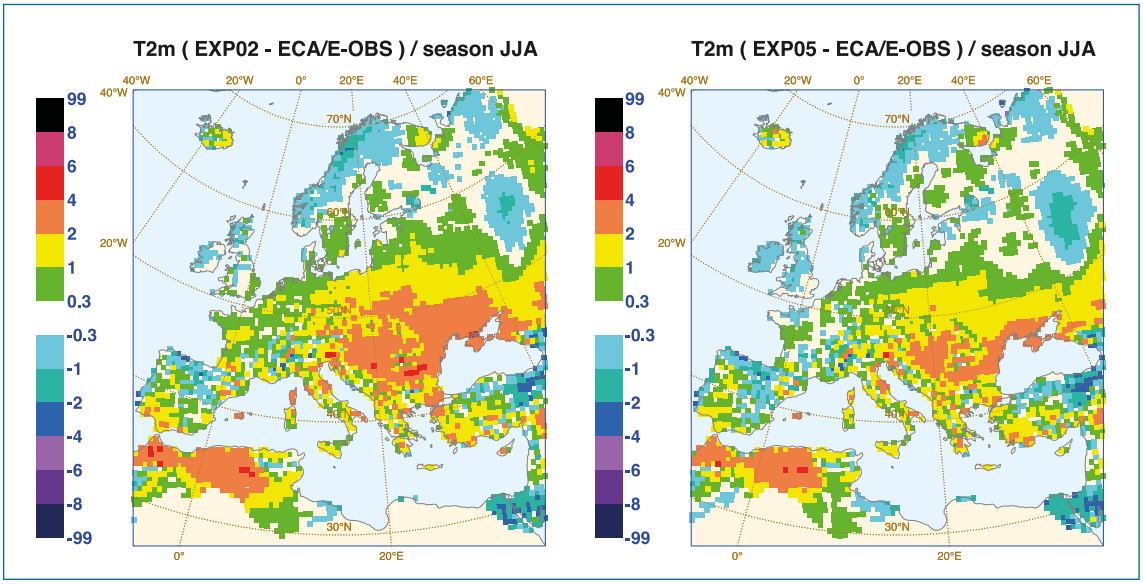

Figure 5.6.2.
Bias in mean summer temperature for the baseline version (EXP02) and a version including HTESSEL, TKE and LAI (EXP05).

One of the aims of developing the soil hydrology parameterization was to reduce the bias in summer temperature in regions with a vegetated surface like Central Europe. Results of experiments EXP06, 07, and 08 are shown in Figure 5.6.3. Focusing on the area of interest, the bias ranges from slightly positive with values beyond 2K in a limited area for the experiment with the water stress function expressed in pressure to a very substantial positive bias with values beyond 4K for the experiment with partially reduced maximum root depth. There is however a catch in the interpretation. In extensive areas of Central and Eastern Europe cropland irrigation is a widely used means to mitigate the results of soil drying when anomalously warm and dry atmospheric conditions prevail for prolonged time. Although it is poorly known how frequent and how widespread irrigation is applied and in what amounts, it is almost certain that the observations in the ECA/E-OBS data set have been affected by irrigation, while the water supply from irrigation is unaccounted for in the model. In a qualitative sense, irrigation plays the same role as a positive soil moisture increment in data assimilation.

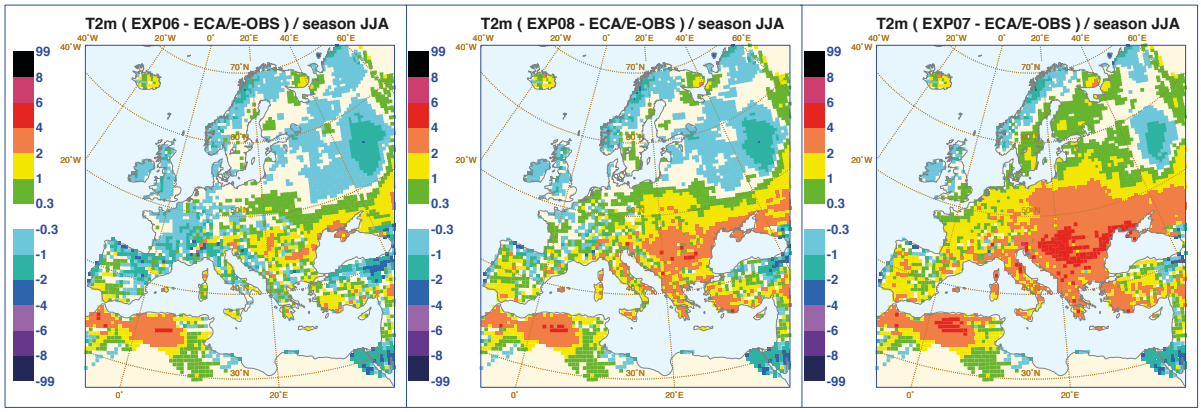

Figure 5.6.3.
Bias in mean summer temperature for the sensitivity experiments on soil hydrology. Shown from left to right are EXP06, EXP08 and EXP07.

The performance is summarized in Figures 5.6.4 (winter) and 5.6.5 (summer) by assessing the bias and the mean standard deviation for all experiments and for a number of regions.

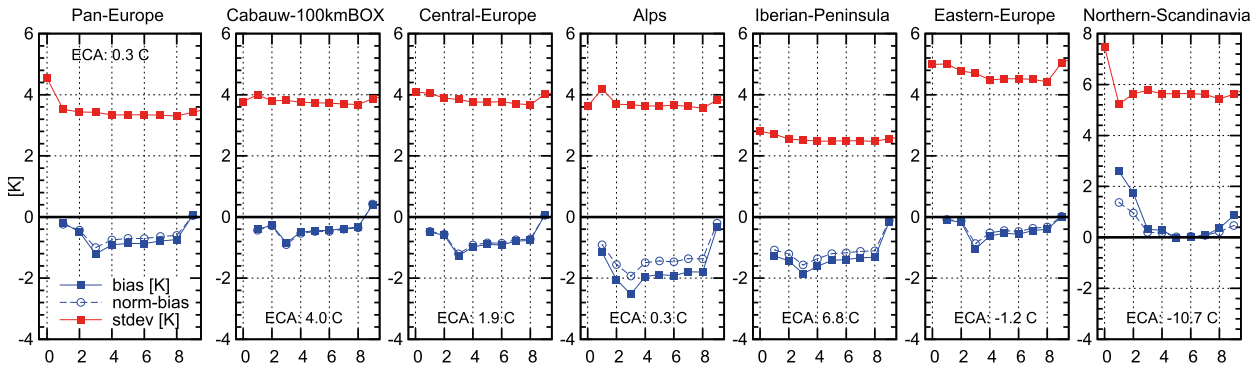

Figure 5.6.4.
Bias (solid blue curve) in daily mean 2-meter temperature in winter (DJF) for experiments described in Table 5.6 for a number of regions in Europe. Normalized bias (dashed blue curve) is defined as the ratio of the bias and the assigned observational uncertainty. The red curve labels standard deviation. The horizontal axis labels the experiments (1-8), the ERA-Interim analysis (9) and ECA (0). In the top-left corner of each of the figures the average ECA value for that region is shown. Cabauw is the experimental site in the Netherlands for in-situ and ground-based remotely sensed atmospheric observations (4.93 E; 51.97 N).

In general, the cy31-based results are colder than the control version (EXP01). For most regions this implies a more negative bias, except for regions in Northern Europe where the considerable positive bias obtained with the control version is greatly reduced in the experiments EXP03-08. The lower temperatures in these experiments result from different modifications in the model formulation. In EXP03 the sub-grid scale vertical mixing in the free troposphere is considerably suppressed leading to reduced boundary-layer top entrainment, increased cloud cover and shallower boundary layers in wintertime. The TKE-formulation employed in EXP04-08 leads to shallower stable boundary layers in wintertime, resulting in an enhanced cloud cover and a lower near surface temperature. The normalized bias compares the bias with the estimated error in observed temperature. The latter parameter is contained in the ECA/E-OBS data set. Absolute values of the normalized bias less

than 1 should be interpreted as not significant. The observed temperature error is estimated to be order 1K except in the Alps and Scandinavia where larger errors are assigned. Biases in mean winter temperature are found only significant for limited combinations of experiments and regions. Finally, the observed standard deviation in winter temperature is reasonably well reproduced, with the exception of regions in Northern Europe where extremely cold events are not adequately captured by the model resulting in an underestimation of the standard deviation.

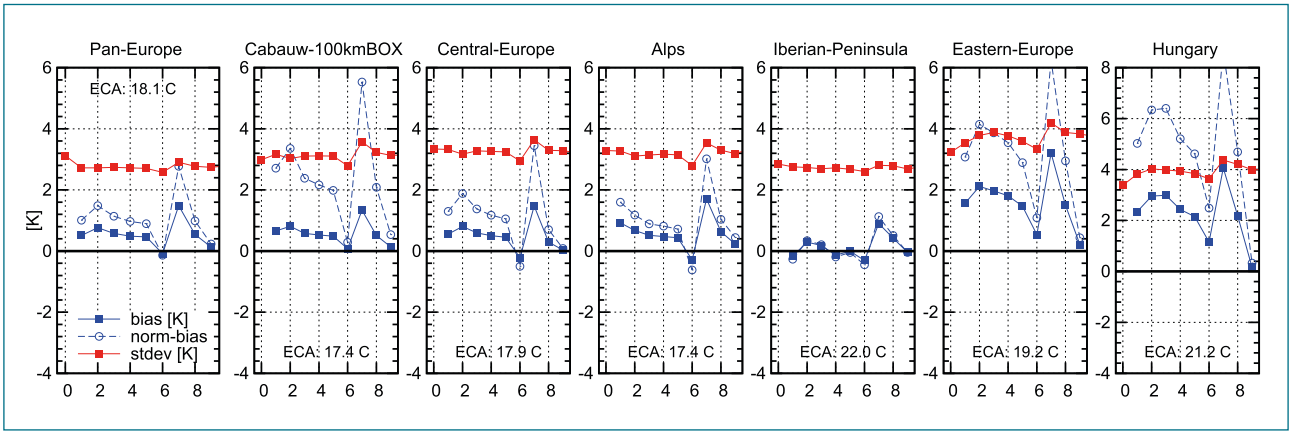

Figure 5.6.5.
Like Figure 5.6.4 but for summer (JJA) (Hungary replaces Northern Scandinavia).

The bias of summertime temperatures is found to be (slightly) positive in most regions with a negligible bias fort the Iberian Peninsula. Model experiment 06 (see table 5.6) is performing best. Since water stress is effectively reduced in this formulation, soil water availability is larger than in the other experiments leading to more evaporation at the expense of sensible heat flux, hence lower temperatures. Replacing the modification on water stress by the use of additional depth classes corresponding to shallower maximum root depths (i.e. experiment 07) results in the worst performing simulation. Shallower roots effectively imply reduced soil water availability since a smaller amount of soil water is directly available for evapo-transpiration, this leads to higher sensible heat fluxes, hence higher temperatures and an even more positive bias compared to the control and reference runs. Also experiment 08 which combines the modifications of experiments 06 and 07 performs worse than experiment 06.

Interestingly, the error assigned to observed temperature in summer is smaller than in winter, which results in a larger number of experiments with a significant bias. The observed standard deviation in summer temperature is reasonably well reproduced with the largest deviation simulated by experiment 07 and the smallest by experiment 06.

Evaluation of minimum and maximum 2-meter temperature

In addition to the evaluation of daily mean temperature it is also very useful to look at the model performance in reproducing the daily temperature extremes. It provides information on the predicted diurnal cycle in temperature compared to observations but it might also give a hint how model performance in predicting mean daily 2-meter temperature should be interpreted. E.g. good skill in mean 2-meter temperature may be the result of opposing compensating errors in predicting daily maximum and minimum temperatures, whereas poor skill might be solely associated to poor skill in only one of them. With that in mind we have combined the biases in minimum and maximum 2-meter temperature in Figures 5.6.6 (DJF) and 5.6.7 (JJA).

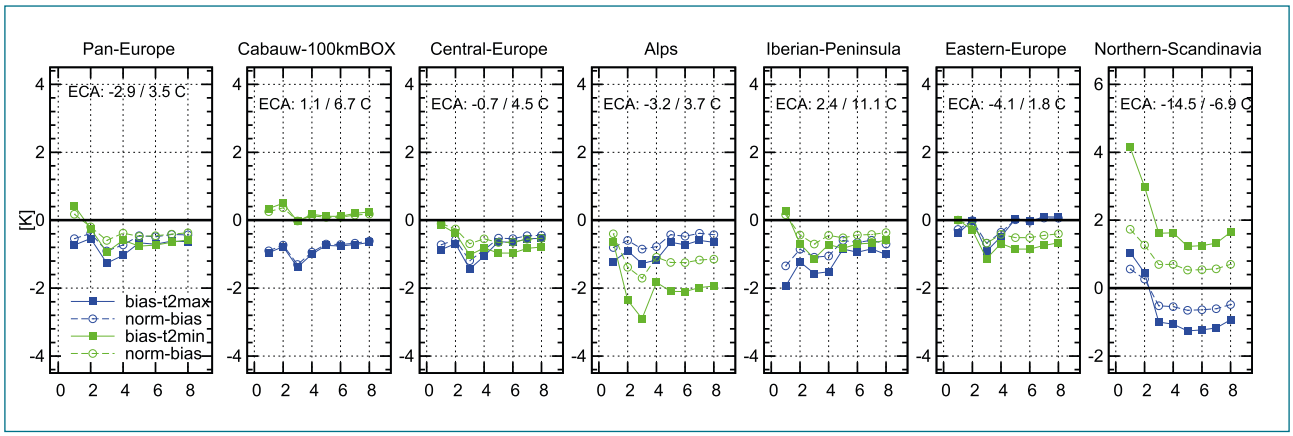

Figure 5.6.6.
Bias (solid curves) and normalized bias (dashed curves) in daily minimum (green) and maximum (blue) 2-meter temperature in winter (DJF) for experiments described in Table 5.6 for a number of regions in Europe. The horizontal axis labels the experiments (1-8); unlike in Figs. 5.6.4 and 5.6.5 the ERA-Interim estimate is lacking.

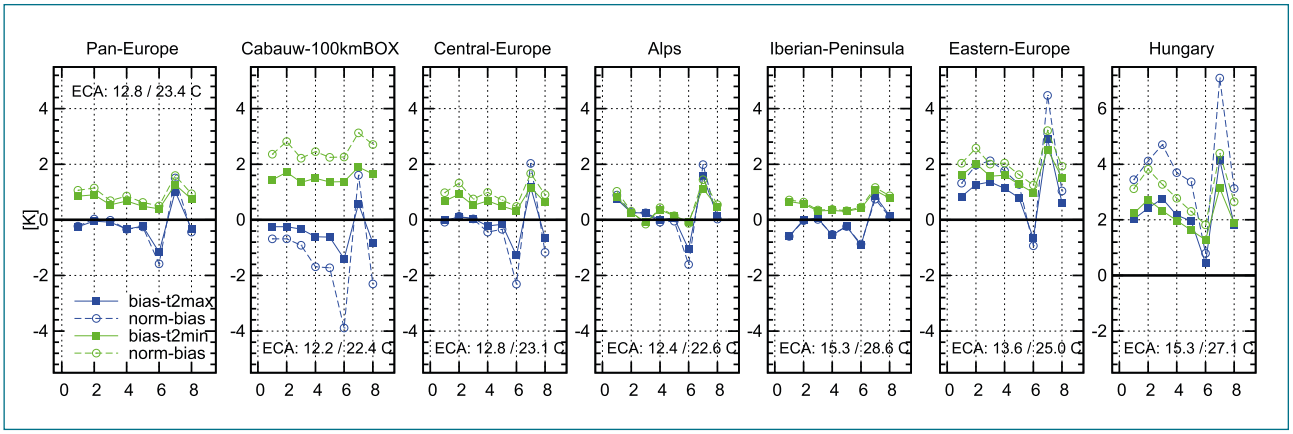

Figure 5.6.7.
Like Figure 5.6.6 but for summer (JJA). (Hungary replaces Northern Scandinavia).

In general the bias in maximum temperature is less positive or more negative than the bias in minimum temperature, the exception for DJF being some of the experiments in Central- and Eastern Europe, and in particular the Alps, and for JJA some of the experiments in the Alps and in particular Hungary. This implies that apart from the exceptions just mentioned all model experiments underestimate the amplitude of the diurnal cycle. For Northern Scandinavia (DJF) and the Cabauw Box (JJA) the biases tend to cancel, the latter with the exception of EXP07. In fact, the smallest bias in JJA in the diurnal amplitude is found for EXP07, implying that for this experiment the entire daily temperature cycle is rather evenly shifted upwards. The opposing example is EXP06 where the negative bias in diurnal amplitude is largest, primarily owing to substantial negative bias in maximum 2-meter temperature. This leads to the uncomfortable conclusion that the good skill in daily 2-meter temperature during JJA obtained with EXP06 is to a large extent the result of compensating errors together with a substantially underestimated diurnal cycle. On the other hand, the substantial positive bias in 2-meter temperature obtained with EXP07 is accompanied by a reasonably good performance in diurnal cycle amplitude.

Evaluation of Precipitation

More so than for temperature the comparison of model predicted precipitation with ECA data yields typical spatial patterns of bias which are hardly different between model experiments. Figure 5.6.8

shows the ECA inferred winter precipitation in mm/day next to the bias in the control version and the baseline version.

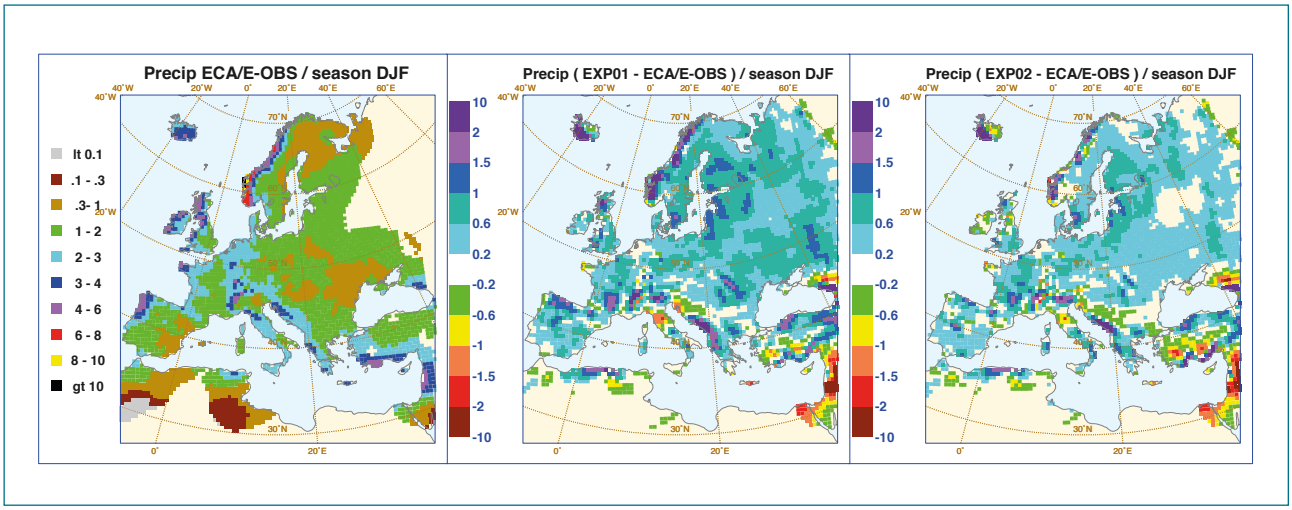

Figure 5.6.8.
Observed mean precipitation in winter and corresponding bias for model experiments EXP01 and EXP02.

Observed mean winter precipitation correlates very strongly with orography superimposed on a background that tends to decrease with distance to the Atlantic Ocean or North Sea. In general, the model overestimates mean winter precipitation by about 0.4-1.2 mm/day. The overestimation in mountainous regions is larger. Of relevance is the finding that the model produces much more frequently than observed measurable precipitation at the daily scale. This feature, nicely seen in Figure 5.6.9, illustrates a very common characteristic among models.

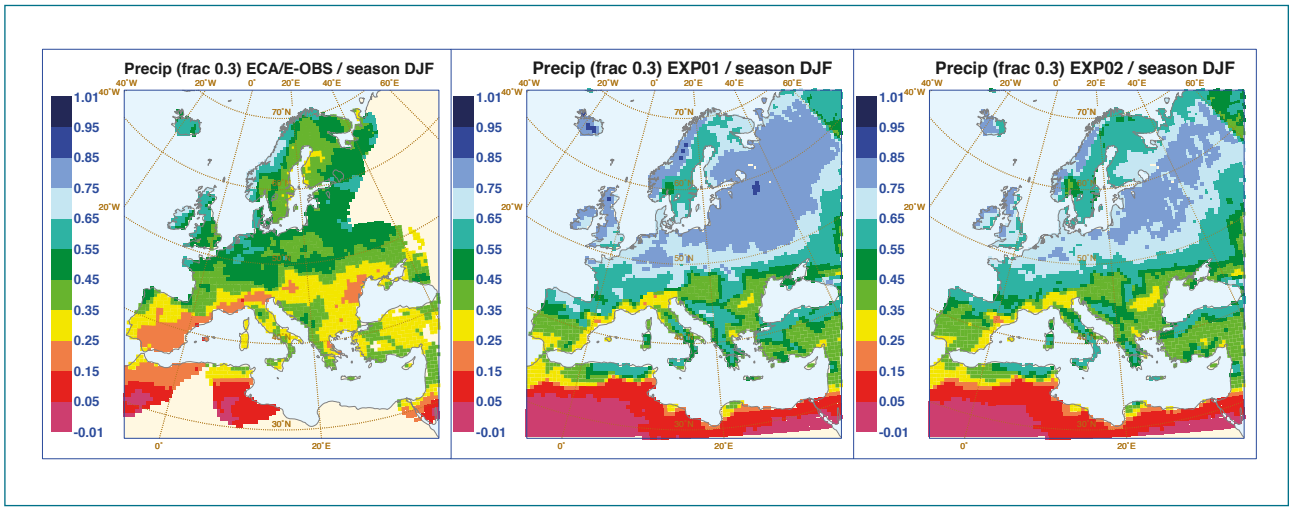

Figure 5.6.9.
Fraction of days in winter with precipitation exceeding 0.3 mm inferred from ECA and derived from EXP01 and EXP02.

Also important is to know whether the model is able to realistically reproduce the observed statistics in large daily amounts. In general, as is shown in Figure 5.6.10 the model seems reasonably capable in simulating the amount of precipitation that corresponds to the 99-percentile (including dry days), but, admittedly, this conclusion can not be extrapolated to more extreme events.

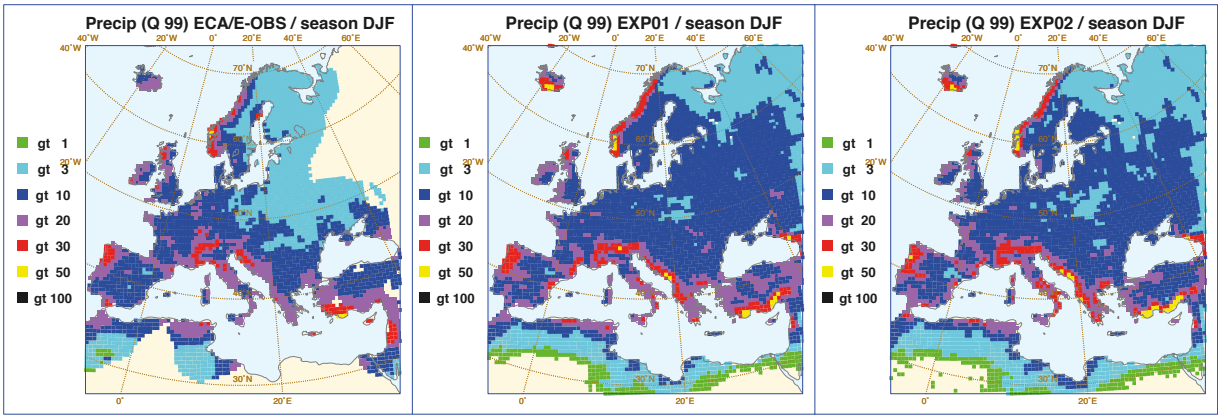

Figure 5.6.10.
Daily amount of precipitation in winter exceeded at the 99-percentile (about the wettest day in winter) inferred from ECA and derived from EXP01 and EXP02.

Like in winter, mean precipitation in summer is largest in mountainous regions as seen in Figure 5.6.11. However, much more so than in winter the Alps are standing out in the amounts of precipitation they receive in summer. Also noteworthy is the decline to virtually no precipitation in the southern Mediterranean. The models show prominent positive biases in Scotland, parts of Scandinavia and also part of Russia, whereas there is a strong underestimation in the region between the Alps and the Black Sea.

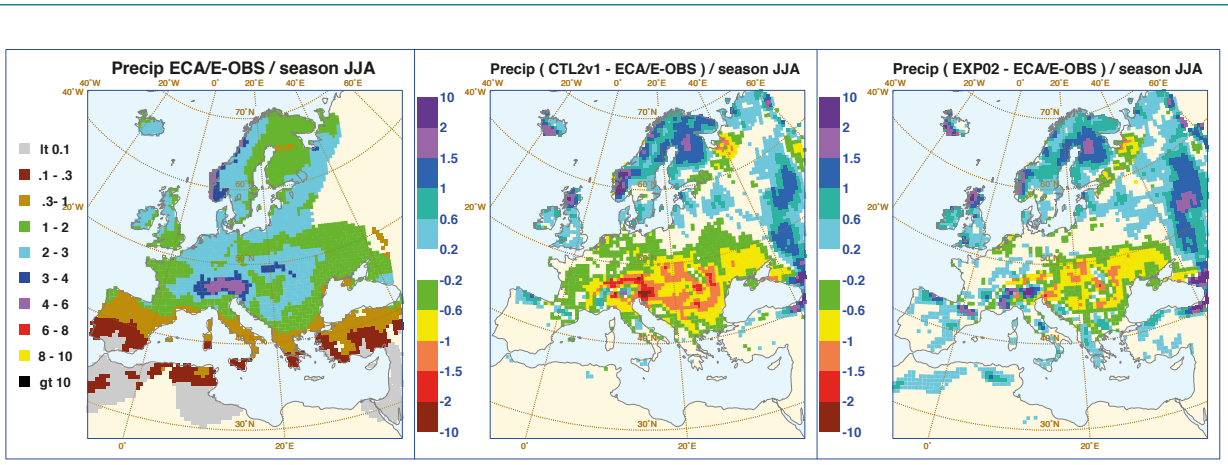

Figure 5.6.11.
Observed mean precipitation in summer and corresponding bias for model experiments EXP01 and EXP02.

Like in winter, the model overpredicts the number of wet days in summer (Figure 5.6.12), however the control version (EXP01) performs clearly better than the baseline version (EXP02). This is most likely related to the modification in EXP01 to enhance the threshold convective depth from 0 to about 1500 m before precipitation is released, which is absent from EXP02.

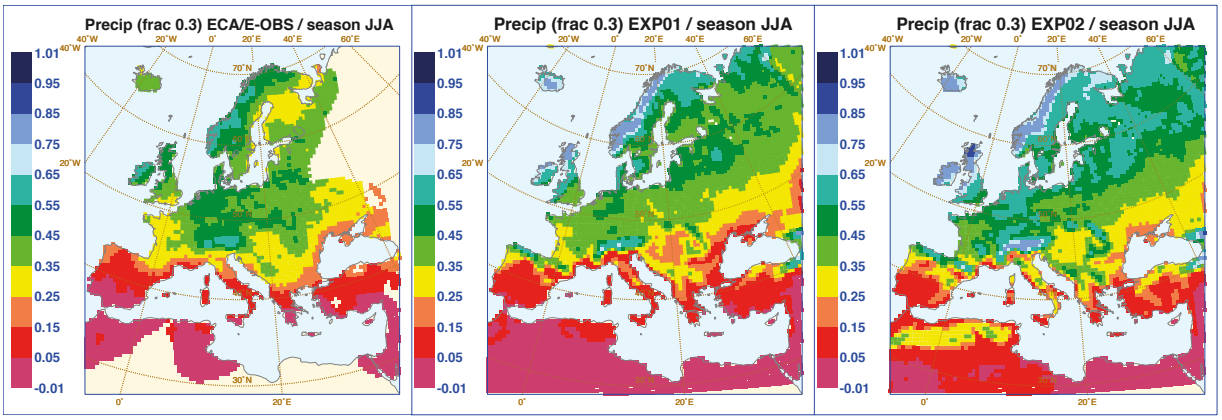

Figure 5.6.12.
Fraction of days in summer with precipitation exceeding 0.3 mm inferred from ECA and derived from EXP01 and EXP02.

Again, like in winter, the ability of the model to reproduce the daily amount corresponding to the 99-percentile in summer is reasonably well although it is by no means perfect. Amounts in Scandinavia are too high, whereas amounts in Central Europe are on the low side. While EXP01 is performing well in the northern Sahara off the coast namely even at 99-percentile amounts below 1 mm/day, for unknown reason EXP02 is considerably overestimating this amount.

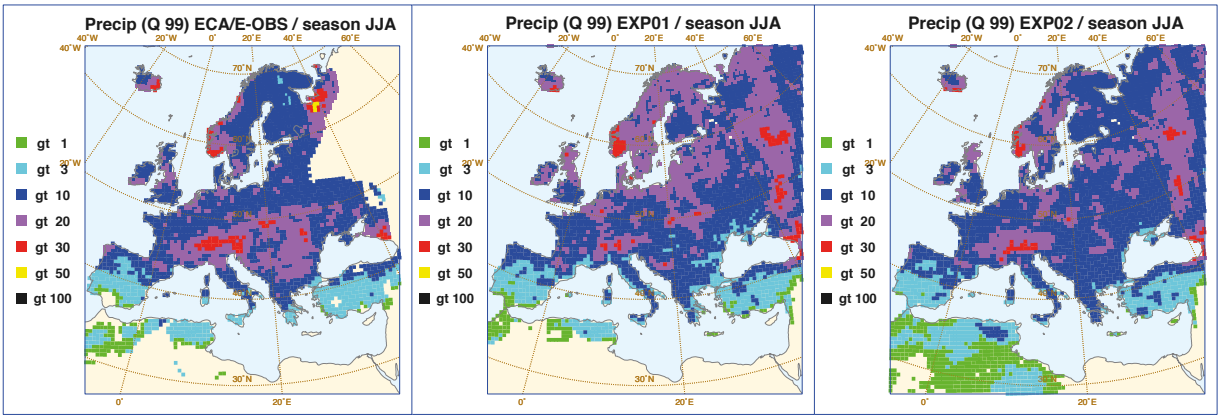

Figure 5.6.13.
Daily amount of precipitation in summer exceeded at the 99-percentile (about the wettest day in summer) inferred from ECA and derived from EXP01 and EXP02.

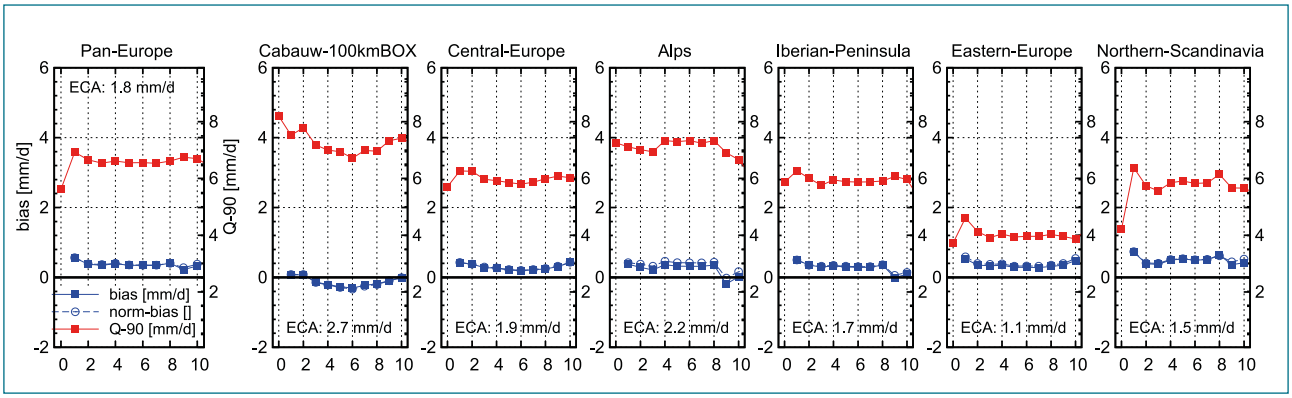

Figure 5.6.14.
Bias (solid blue curve) in daily mean precipitation in winter (DJF) for experiments described in Table 5.6 for a number of regions in Europe. Normalized bias (dashed blue curve) is defined as the ratio of the bias and the assigned observational uncertainty. The red curve labels the 90-percentile of region-averaged sorted amounts. The horizontal axis labels the experiments (1-8), the ERA-Interim analysis (9,10) and ECA (0) Results for 9 and 10 are derived from t+00-t+12 and t+12-t+24 forecasts, respectively, within the ERA-Interim cycle.

Biases in mean winter precipitation are generally positive (see also Figure 5.6.8) but small, in the order of 0.4 mm/day or less. This even holds for a mountainous region like the Alps. For the Norwegian mountains the biases are somewhat larger (not shown), in the order of 0.6-1.0 mm/day, which is however still less than the assigned observational error. The experiments we have conducted show very little sensitivity in this variable. A similar conclusion can be drawn for P(Q=90) indicating the amount of region-averaged precipitation that corresponds to the 90-percentile, although in some regions the model simulated values tend to be somewhat further off the observed values.

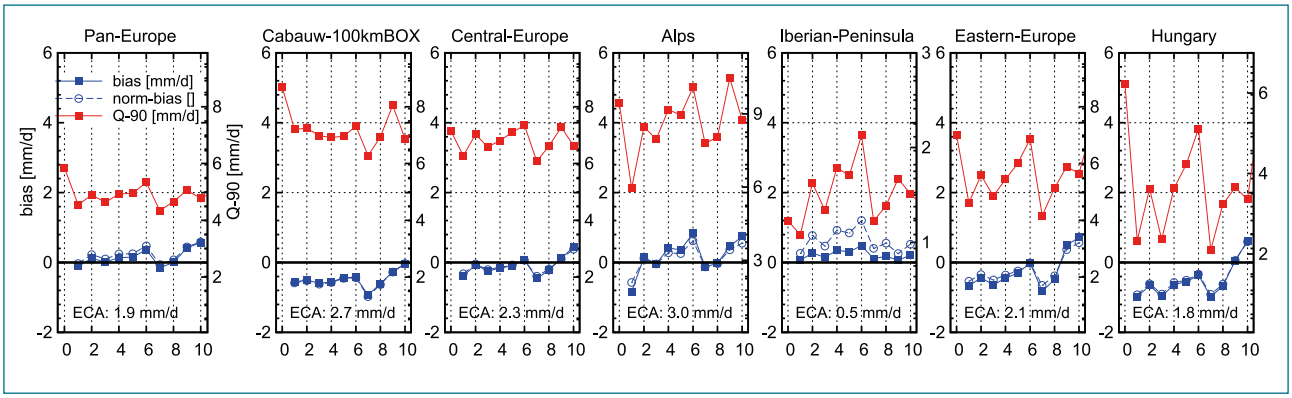

Figure 5.6.15.
Like Figure 5.6.14 but for summer (JJA) (Hungary replaces Northern Scandinavia).

Simulated summer precipitation shows more variation among the experiments that were carried out. For most regions, the control version (EXP01) and the sensitivity experiment with varying root depth class (EXP07) had lowest mean summer precipitation while the sensitivity experiment with pressure head dependent water stress (EXP06) produced the highest summer precipitation. The same holds for P(Q=90). In most regions, but not all (Alps, Iberian-Peninsula) EXP06 performs best in reproducing parameters characterizing summer precipitation.

5.7 Conclusion

In this chapter we evaluated a variety of model experiments with a high resolution gridded data set of daily values of temperature and precipitation. All experiments were conducted in the same framework, meaning same domain, same spatial resolution (50km), same 8-year integration period (2000-2007), and same forcing (ERA-Interim). The purpose of the evaluation is to quantify the differences in performance among the various model formulations in order to be capable of objectively establishing a final, so called frozen version of RACMO2.2, supposedly applied in next generation climate scenario calculations. Modifications in model formulation were restricted to changes in the model physics and all built from a baseline version of RACMO2.2. This version, referred to as the reference, was adopted by porting the entire physics package from the ECMWF model cycle31r1 into RACMO2. The frozen version of RACMO2.1 served as a control version.

The baseline version and the control version differ in many aspects as was already pointed out in paragraph 5.2. Modifications to the baseline version only affected the boundary layer scheme or the soil moisture component of the land surface scheme. If for a given parameter or for a given region the baseline version performs worse than the control version for reasons that can not be identified with either of the two schemes, the modified versions can not be expected to yield an improved skill. Because of massive changes in coding infrastructure it was found very difficult to back substitute new elements in version 2.2 with old elements of version 2.1 when a certain degrading in performance could be attributed to the new elements. Perhaps this would also be an undesirable action.

The primary conclusion is that there is no best model formulation that outperforms all other formulations for all parameters and all regions. Rather the opposite holds, that is that differences in performance are marginal, and in particular, improvement in performance in one region is found along with degrading performance in other regions. Keeping this in mind the main conclusions are:

- The performance of the control version is already of high quality and difficult to improve. In fact, a recent study demonstrated that RACMO2.1 is currently (by far) the best performing European regional climate model (Christensen et al., 2010).
- The control version appears to be rather smooth compared to observations, and also compared to the versions based on cycle31 physics.
- The large positive bias in Northern European winter temperature found in the control version is very substantially reduced in all formulations employing a TKE-based boundary layer formulation.
- The positive bias in Central European summer temperature found in the control version continues to exist or is even amplified in most of the cycle31 based formulations. A weakening of the positive bias is only obtained with a formulation including HTESSEL in combination with rephrasing of the water stress function (EXP06).
- With a few exceptions the bias in maximum temperature is less positive or more negative than the bias in minimum temperature, implying that in most regions most model versions underestimate the diurnal cycle. EXP06 largely underestimates the diurnal cycle during JJA as opposed to the small bias in representing daily mean temperature in summer. The reverse holds for EXP07. This points to compensating errors.
- In most regions EXP06 provides a favourable performance in reproducing summertime precipitation.
- Wintertime precipitation is reasonably well described in all model experiments and biases are not significant.

6. First Aerosol Indirect Effect at Regional Scale

6.1 Introduction

According to the latest IPCC assessment reports the role of aerosols continues to be a major uncertainty in quantifying future climate change. One can distinguish between the aerosol direct effect, which refers to the process of direct interception of solar radiation by aerosols, and the aerosol indirect effect, which refers to the process whereby the cloud characteristics are altered by the presence of aerosol particles. The primary impact of the direct effect is enhanced atmospheric absorption of solar radiation at the cost of transmission to the Earth's surface and, to a lesser extent, reflection back into space. The primary impact of the aerosol indirect effect (AIE) is more involved. In essence, aerosols are likely to increase the number of cloud condensation nuclei, which favours the formation of more, but smaller cloud particles, hence the effective cloud droplet size (or cloud crystal size) will be reduced. This has two primary but independent effects. The reflectivity of the clouds increases as small particles reflect more radiation than large particles. This directly affects the radiation budget, and is referred to as the first aerosol indirect effect. Also, since cloud particles are smaller the process of precipitation formation is delayed or even inhibited, which leads to longer cloud life times. This process is referred to as the second aerosol indirect effect.

6.2 Model development associated to First Aerosol Indirect Effect

In this project we have examined the impact of the first AIE to climate parameters like temperature, precipitation, cloud amount and global radiation. The tools for this investigation have been developed in collaboration with project CS4. A key component of the instrumentation is formed by the chemistry-transport model LOTOS-EUROS (Schaap et al., 2008). It is used for modelling of aerosol formation, destruction and transport. The meteorological conditions are provided by RACMO, while the calculated 3D distributions of aerosols are returned to RACMO. First we only considered sulphate and fine sea salt, later we added nitrate. Because RACMO and LOTOS-EUROS do not operate on the same grid, couplers were developed to map the information back and forth. The coupling time step is typically 3 hours. Once the aerosol information from LOTOS-EUROS is imported into RACMO the aerosol mass concentrations are converted into number concentrations of Cloud Condensation Nuclei (CNN). For this we applied the relatively simple parameterization by Menon et al. (2002) It gave the best result in a comparison study conducted in CS4 (de Martino et al., 2008), it is easy to implement in the RCM and it could be straightforwardly extended with nitrate. The CNN amounts are subsequently combined with the RACMO simulated liquid water contents to determine the corresponding effective radius which is the primary model parameter in controlling the interaction between clouds and solar radiation. Rather than using the in-situ value of cloud liquid water content at every model level we applied a mixing model to specify an in-cloud liquid water profile derived from liquid water content at model base. This method provides a more robust and likely also more realistic estimate of an in-cloud profile of effective radii. Finally, since a RACMO grid box might contain multiple sub-grid scale cloudy columns with different cloud base levels, the effective radii at a given level coming from different cloudy columns have to be combined in a single value of the effective radius. This is done by weight averaging the effective radii with the weight being the ratio of the areal fraction of the cloudy column relative to the grid-box mean cloud cover. The averaged effective radius, only obtained in this way for liquid water clouds, is then used to account for the cloud radiation interaction at that level.

6.3 Impact of the First Aerosol Indirect Effect

To explore the sensitivity of the impact of the first aerosol indirect effect to climate change we carried out a climate scenario calculation (1970-2060) with RACMO coupled to LOTOS-EUROS. Atmospheric forcings and sea surface boundary conditions were taken from ECHAM5. The horizontal resolution was set to 50km, while the RACMO domain was adapted to just envelop the LOTOS-EUROS domain (see Figure 6.3.1, left panel). A constant annual cycle was imposed to the emission sources during the full integration. A likewise configured but uncoupled RACMO integration served as reference. Yet, in the reference the indirect aerosol effect is implicitly brought into account by applying a diagnostic formulation of the effective radius of liquid water cloud particles derived from cloud liquid water content and prescribed fixed concentrations of cloud condensation nuclei over land and sea (Martin et al., 1994). In the coupled run, the latter formulation is employed outside the LOTOS-EUROS domain. Figure 6.3.1 (right panel) show the size distributions of the effective cloud droplet radius sampling one month of integration and utilizing either of the two effective radius formulations.

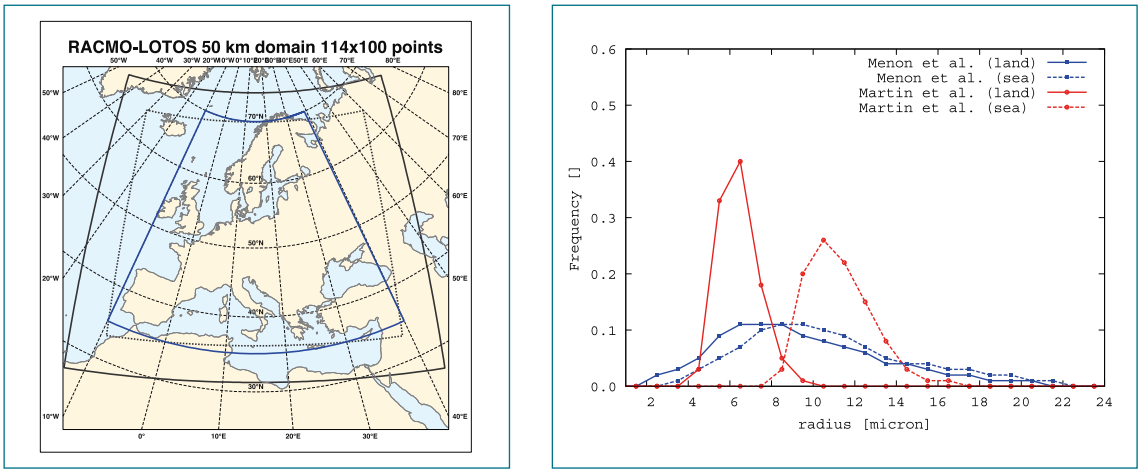

Figure 6.3.1.
(left panel) RACMO domain (solid black line) and LOTOS domain (blue line) in coupled integration. Dashed black line marks transition between boundary relaxation zone and interior domain in RACMO (left panel). Effective droplet size distributions inferred from RACMO utilizing the Martin et al. (1994) formulation in the uncoupled run and the Menon et al. (2002) formulation in the coupled run for June 2006. Effective radius values only contributed to the distribution for layers with liquid water content exceeding a threshold of 10^{-4} kg/kg.

In the coupled run the median effective radius over land is found at about 8 μ over land and 9 μ over sea. In the uncoupled runs, these values are 6 μ and 11 μ, respectively, which implies a much larger contrast between land and sea. It is furthermore remarkable that the distributions in the coupled run are much wider than in the uncoupled run, which is likely the result of explicit spatially heterogeneous aerosol loading in the coupled simulation. Assuming that these frequency distributions are representative for the full integration – and there is no reason to assume they are not – we expect in lowest order that the short wave radiation incident at the surface in the coupled run is somewhat larger than in the uncoupled because of enhanced in-cloud transmissivity associated with larger cloud droplets. The overall effect on other parameters like e.g. 2-meter temperature of course depends on many other factors like cloud amount, the presence of ice clouds and the relative importance of short wave radiation on the surface energy balance. The largest effect is expected in snow free land regions during summer with high amounts of optically thin or modest liquid water clouds not shielded by ice-clouds. Results for short wave incoming radiation at the surface and 2-meter temperature are shown in Figs. 6.3.2. The figure contains difference plots between the results from the coupled and the uncoupled run – the impact of an explicit versus an

implicit account of the first indirect aerosol effect – and between 30-year mean fields in a future climate (2031-2060) and in present-day climate (1971-2000) – the effect of climate change.

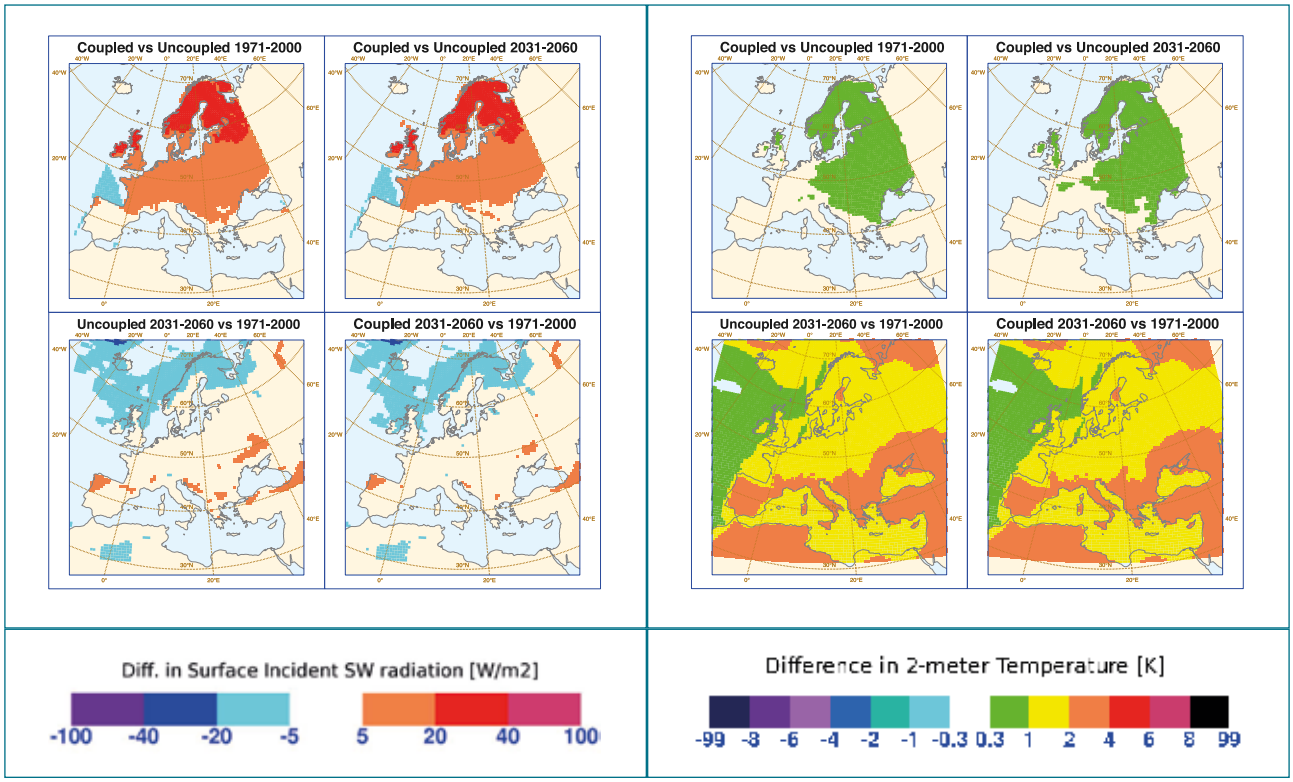

Figure 6.3.2.
Difference in surface incident short wave radiation (left 4 panels) and 2-meter temperature (right 4 panels) between the uncoupled and the coupled run for both periods of integration (top row), and between a future 30-year period and the present-day 30-year period for both runs (bottom row). All plots are valid for JJA. The difference in climate change between the coupled and uncoupled run follows from comparing the plots in the second (fourth) column with those in the first (third) column.

Differences in surface incident short wave radiation between the two experiments (coupled minus uncoupled) are substantial in Central Europe and, in particular, in Northern Europe, where 30-year mean differences are between 20 to 40 Wm^{-2}, which amounts to 10-20%, in some regions to 30% of the total monthly mean. Differences over land are always positive which is consistent with Figure 6.3.1. Over sea differences are small, whereas in Southern Europe mean differences are negligible which is of course consistent with the very low cloud amount in summertime in this part of Europe. The effect on 2-meter temperature is very modest with a small temperature excess of less than 1 K in Eastern and Northern Europe. Hence the temperature impact of the first indirect aerosol effect is considerably smaller than the anticipated increase in temperature corresponding to climate change. On the other hand, the calculated climate change effect over land to incident surface short wave radiation is small (absolute difference less than 5 W m^{-2}) in Northern Scandinavia and some patchy areas across Southern Europe, for the rest it is negligible (less than 5 W m^{-2}). Moreover, the climate change patterns are found to be amazingly similar for the two experiments, implying that in the framework of this climate scenario calculation the impact of the first indirect aerosol effect is virtually insensitive to climate change.

7. Conclusions / synthesis, recommendations, outlook

In the preceding chapters we have provided an overview of the research carried out within project CS6 since 2005, some of it in close collaboration with CS3, CS4 and CS5, and discussed in detail the results and obtained insights. In the final chapter we want to summarize the main achievements of the CS6 project and formulate an outlook of possible next steps that raise our knowledge and infrastructure to a next level that best meets the requirements of (near) future applications. In particular, we will address the question how the upgraded regional climate model system is going to contribute to the next generation of climate scenario's, and what components still need attention to improve the usefulness.

In the first phase of the project we carried out a climate scenario calculation with the existing KNMI regional climate model version RACMO2.1, an effort also in contribution to the EU-ENSEMBLES project. The integration was covering all of Europe for the period 1950-2100, driven by the ECHAM5-GCM and using green house gas concentrations according to SRES-A1B emission scenario (see Figure 2.1).

In a latter stage of the project a second climate scenario calculation with RACMO2.1 was carried out in exactly the same configuration but forced with boundary conditions from the Japanese GCM MIROC3.2 highres. The two GCMs exhibit significantly different climate change patterns, where both are a priori equally plausible(see Figure 2.2). With this example we emphasize that users of RCM-produced climate change patterns with high spatial detail should be constantly aware that keeping the RCM but replacing the forcing GCM will retain that amount of detail but might radically change the pattern of the detail.

The performance of regional climate models can be analyzed in many ways. In this report we presented a few examples, among them the role of North Sea surface temperatures to summertime in-land precipitation in The Netherlands, and the relation between extreme precipitation and temperature hourly and daily time scales. Also we discussed an application in which wind speed time series produced by the climate scenario calculation are used to drive a surge model with the aim of establishing the climate change signal in the return time of the annual maximum wind-induced water level height along the Dutch coast.

Concerning the role of North Sea surface temperatures we analyzed the month of August 2006 which was characterized by persistent cool and unstable atmospheric maritime conditions following a record breaking warm month of July. Because of that, North Sea temperatures were anomalously high in August, especially in the beginning of the month. RACMO, for this purpose operated at a very fine 6 km resolution, was found very well capable of producing the high amounts of precipitation that had been observed, while from sensitivity experiments it was also made plausible that high sea surface temperatures had indeed contributed to the excessive amounts of precipitation. Yet, this study also revealed the limitations of RACMO. Firstly, observations clearly showed that the maximum intensity in precipitation occurred in-land about 30 to 50 km off the coast, whereas the model persisted in releasing the precipitation in the grid boxes adjacent to the coast line. In our view this shortcoming is associated with the parametric representation of deep convection, the use of which is standard practice in hydrostatic formulations. This approach does not allow the time evolution of an organizing meso-scale convective system that reaches its mature stage some time after the convection has been triggered, during which the system might have travelled inland. This assumption might very well be investigated by applying an atmospheric model employing non-hydrostatic dynamics and resolved convection.

Secondly, observations show that the anomalously high sea surface temperatures are limited to a very narrow tongue off the coast, yet they have a profound effect on inland precipitation. In order to capture this small-scale regional effect in a climate scenario calculation requires that the model is capable of predicting its own sea surface temperature at full model resolution rather than diagnosing it from – what is customary practice – the forcing GCM operated at coarse resolution. This requires an additional model component, e.g. an ocean slab model, in which the sea surface temperature can be accurately estimated by combining heat exchanges with the atmosphere and deeper water together with contributions from horizontal heat transport. This work is being carried out in the context of the follow-on KfC program.

Analysis of multi-year records of hourly precipitation indicates robustly that hourly amounts corresponding to the most intense precipitation events (at the 99.9% level) increase by 14% per degree temperature rise, which is twice as high as expected from arguments based on Clausius-Clapeyron. The enhanced rise is seen in the higher temperature range in which precipitation is primarily produced by convection. An underlying mechanism to explain the observed behaviour has not been established yet, though there are indications that both absolute and relative humidity act as steering parameters. Interestingly, some of the RCMs that participated in EU-ENSEMBLES, including RACMO, show similar scaling behaviour, which also appears as a strong climate change signal of enhanced extreme amounts of the most intense events in a warmer climate. However, as long as a proper explanation is lacking it remains unclear whether the models show the right behaviour for the correct reason. To settle this issue evidently more research is needed, preferably with the combined use of conceptual models to gain understanding and cloud resolving models to quantify the process.

From applications of RACMO in representing high wind speeds associated with synoptic-scale storms two relevant conclusions can be drawn. Firstly, the model is very well capable of reproducing the evolution of these storms, provided it is forced with proper lateral boundary conditions. Increasing the horizontal resolution does result in more refinement, as expected, which might be very useful in the vicinity of land sea transitions. However, it does not affect the character of the wind speed – e.g. wind speed extremes, areal size with high wind speeds, etc. – nor does it alter the large-scale features of the storm when compared to results obtained at coarser resolution. Secondly, from a multi-annual climate change calculation it is derived that in terms of return times of annual-maximum daily mean wind speed RACMO confirms what is (already) found in the driving GCM ECHAM5 and other GCMs, which is consistent with the first conclusion. Differences in this comparison are thought to be ascribed to the use of slightly different parametric assumptions in the high wind speed regime.

A considerable effort was made in model development. The RACMO model physics has been upgraded with ECMWF physics from cycle31r1. Various components from this baseline version have been further developed. The boundary-layer mixing scheme has been replaced by a unified scheme which combines two existing schemes, i.e. a moist mixing scheme based on turbulent kinetic energy (TKE) to account for vertical transport due to turbulent mixing, and a dual mass flux scheme to account for vertical transport due to organized shallow convection. Overall, the new scheme results in a better representation of the stable boundary layer and the day-time convective boundary layer. In a separate effort, much focus was put on the soil hydrology component of the model. Spatially homogeneous soil hydrology parameters from TESSEL have been substituted by spatially heterogeneous parameters from HTESSEL, adopted from cycle33r1. Additional modifications to HTESSEL that have been tested include the use of spatially varying maximum root depth and root water uptake reduction controlled by soil water pressure head instead of soil moisture content. Also a seasonally varying leaf area index (LAI) inferred from some years of MODIS observations has been introduced to replace the constant field inferred from ECOCLIMAP.

The alternative model versions have been thoroughly tested in climate mode against high resolution gridded daily observations on temperature and precipitation compiled within the ECA/E-obs data set for the purpose of model evaluation. All experiments were integrated over an 8-year period (2000-2007) at 50 km resolution. The main findings are that the transition from the control version (RACMO2.1) to the baseline version built on cy31r1 physics deteriorates the performance. It requires the collective introduction of the TKE-based boundary-layer scheme, seasonally varying LAI, and HTESSEL, to come to a model version that performs comparable to the control version. Thus, it is difficult to improve the control version, which seems compatible with the finding that RACMO2.1 is a very good model, scoring (by far) best in an inter-comparison between 15 European climate models (Christensen et al., 2010). Exceptions are the model skill in representing temperature in persistent stable conditions that occur during winter in Scandinavia which is found significantly improved owing to the TKE-formulation. Also the introduction of spatial heterogeneity in HTESSEL results in more small-scale spatial features which better resemble the observed patterns.

The two modifications in the model soil hydrology component developed and implemented in project CS3 have opposing effects to the model behaviour, both primarily in spring and summer, but partly in distinct regions. On the one hand, making the root water uptake reduction function dependent on pressure head instead of volumetric soil moisture content, the former considered more physically sound, essentially enhances soil water availability in all vegetation covered areas for a wide range of soil water values. Hence, it favours evapo-transpiration at the expense of sensible heat flux, resulting in lower near surface temperatures. On the other hand, introducing reduced maximum root depth in areas with predominantly rocky or stony soils effectively reduces the soil water availability, hence lowers the evapo-transpiration, which leads to higher near surface temperatures. Each of the modifications applied separately yields a distinctly poor performance in either the mean diurnal cycle or the mean daily temperature. But even applied in combination the effect to the performance is more or less neutral when considering larger regions, which is somewhat of a disappointing outcome. It underlines how difficult it is to transfer improvements in model formulation which are introduced for good reasons into a better performing model. In many cases this is owing to compensating model errors, but it may also often be attributed to the fact that a process is misrepresented in the model or not represented at all.

The frequent and widespread application of irrigation in agricultural areas during dry episodes in spring and summer seriously hampers the interpretation of the temperature evaluation. Qualitatively, irrigation will have a cooling effect, but the size of the cooling is difficult to quantify without knowing the intensity of the irrigation. Since all model experiments are carried out without simulating the effect of irrigation it is a plausible assumption that the model temperature bias in summer should in fact be positive, however to what extent is unclear. In the final report of project CS3, van Dam et al. (2011) discuss in more detail the role of irrigation.

Much progress has been made in extending RACMO with tools to account for the effect of interactive aerosol. In collaboration with project CS4 (ten Brink et al., 2012) modules have been developed, implemented and tested which describe the transformation from the mass densities of various types of aerosols (sulphate, nitrate, fine sea salt) into cloud condensation nuclei numbers and the associated cloud droplet effective radius. This enables the computation of the first indirect aerosol effect. Moreover, RACMO was coupled to the chemistry-transport model LOTOS-EUROS to allow high-frequency exchange of information. Typically every 3 hours atmospheric parameters are transmitted forth to force the chemistry-transport model while aerosol fields are transmitted back to be fed into the climate model. This strong coupling guarantees that both models experience the same atmospheric structures. As proof of principle the coupled system has been applied in a climate change study keeping emission scenario fixed. It shows the impact of aerosol due to the first aerosol

indirect effect is small but detectable, relative to an arbitrarily chosen reference. However, within the framework of the model study, the effect of climate change to the impact of aerosol was found negligible. Evidently, this type of development on RACMO is not completed yet, since the account of two other important aerosol effects, the direct effect and the second indirect effect, have so far not been considered. Fortunately, already progressing initiatives are taken within CcSP succeeding programs like KfC and NMDC to carry out the necessary steps to incorporate the additional aerosol effects.

Finally, we discuss how the upgraded regional climate model is going to contribute to the next generation of climate scenario's in general, but in particular for the Netherlands, and what components need attention to optimize the contribution. Probably the most prominent potential asset of an RCM is its ability to simulate credible estimates of precipitation, in particular extreme precipitation, and their distribution in space an time. Next to this the model must be capable to provide realistic and consistent estimates of other parameters like temperature, humidity wind, cloud amount, radiation, etc. RACMO has proven to meet these requirements for resolutions in the 10-50km range. The next climate scenarios for the Netherlands will likely distinct between larger regions, e.g. north and south or coastal and interior. We have learned in this project that we need an interactive account of surface temperatures of the shallow North Sea to let the model realistically produce high amounts of precipitation in the coastal zone. Work on this extension of the model is in progress. However, correct localization of high precipitation intensity associated to convection can not be obtained with the present model formulation owing to the use of parameterized convection. Concerning the issue of quantifying the role of aerosols in present-day and future climate by using the regional climate model substantial steps forward have been made. The process representing the first aerosol indirect effect has been included in the model, while a fully high-frequent coupling between RACMO and the chemistry-transport model LOTOS-EUROS has been established. Efforts are currently made to include the processes representing the direct aerosol effect and the second aerosol indirect effect explicitly controlled by interactive aerosol.

References

Baas, P., S.R. de Roode & G. Lenderink, The Scaling Behaviour of a Turbulent Kinetic Energy Closure Model for Stably Stratified Conditions, 2008. Bound.-Layer Meteorol., **127**, 17-36 doi:10.1007/s10546-007-9253-y.

Balsamo, G., P. Viterbo, A. Beljaars, B.J.J.M. van den Hurk, M. Hirschi, A. Betts & K. Scipal, 2009: A revised hydrology for the ECMWF model: Verification from field site to terrestrial water storage and impact in the Integrated Forecast System. J. Hydrometeor., **10**, 623-643, doi:10.1175/2008JHM1068.1.

Brink, H. ten, R. Boers, R. Timmermans, M. Schaap, E. van Meijgaard & E.P. Weijers, 2012. The impact of aerosols on regional climate. CcSP Final Report, KvR **052/12**, 20 pp.

Christensen, J. H., E. Kjellström, F. Giorgi, G. Lenderink & M. Rummukainen, 2010. Assigning relative weights to regional climate models: exploring the concept. Climate Research, 44,179-194. doi:10.3354/cr00916

Dam, J.C. van, K. Metselaar, L. Wipfler, R.A. Feddes, E. van Meijgaard & B. van den Hurk, 2011. Soil moisture and root water uptake in climate models. CcSP Final Report, KvR **017/11,** 60 pp.

Dee, D.P., and 35 co-authors, 2011. The ERA-Interim reanalysis: configuration and performance of the data assimilation system. Q. J. R. Meteorol. Soc., **137**, 553–597. doi: 10.1002/qj.828.

De Martino, G., B. van Ulft, H. ten Brink, M. Schaap, E. van Meijgaard & R. Boers, 2008. An aerosol-cloud module for inclusion in the KNMI regional climate model RACMO2. KNMI publication: WR-**2008-05**, 11/2008.

Haylock, M.R., N. Hofstra, A.M.G. Klein Tank, E.J. Klok, P.D. Jones & M. New, 2008. A European daily high-resolution gridded dataset of surface temperature and precipitation for 1950-2006. J. Geophys. Res., **113**, D20119, doi:10.1029/2008JD010201.

Hazeleger, W., & 31 co-authors, EC-Earth: A Seamless Earth-System Prediction Approach in Action. Bull. Amer. Meteor. Soc., 2010, **91**, 1357-1363, doi:10.1175/2010BAMS2877.1.

Jung, Th., E. Klinker & S. Uppala, 2003. Reanalysis and reforecast of three major European storms of the 20th century using the ECMWF forecast system. ECMWF ERA-40 Project Report Series No **10**.

Knyazikhin, Y., J. Glassy, J. L. Privette, Y. Tian, A. Lotsch, Y. Zhang, Y. Wang, J. T. Morisette, P. Votava, R.B. Myneni, R. R. Nemani & S. W. Running, 1999. MODIS Leaf Area Index (LAI) and Fraction of Photosynthetically Active Radiation Absorbed by Vegetation (FPAR) Product (MOD15) Algorithm Theoretical Basis Document.
http://modis.gsfc.nasa.gov/data/atbd/atbd_mod15.pdf

Lenderink, G. & E. van Meijgaard, 2008. Increase in hourly precipitation extremes beyond expectations from temperature changes.
Nature Geoscience, 1, 511-514, doi:10.1038/ngeo262.

Lenderink, G., E. van Meijgaard & F. Selten, 2009. Intense coastal rainfall in the Netherlands in response to high sea surface temperatures: analysis of the event of August 2006 from the perspective of a changing climate. Clim. Dyn., **32**, 19-33, doi:10.1007/s00382-008-0366-x.

Martin, G.M., D.W. Johnson & A. Spice, 1994. The measurement and parameterization of effective radius of droplets in warm stratocumulus clouds, J. Atmos. Sci., 51, 1823-1842.

Meijgaard, E. van, L.H. van Ulft, W.J. van de Berg, F.C. Bosveld, B.J.J.M. van den Hurk, G. Lenderink & A.P. Siebesma, 2008: The KNMI regional atmospheric climate model RACMO, version 2.1. KNMI Technical Report **302**, 43 pp.

Menon, S., A. D. Del Genio, D. Koch & G. Tselioudis, 2002. GCM Simulations of the Aerosol Indirect Effect: Sensitivity to Cloud Parameterization and Aerosol Burden, J. Atmos. Sci., **59**, 692-713.

Neggers, R.A.J., M. Koehler & A.C.M. Beljaars, 2009. A dual mass flux framework for boundary layer convection. Part I: Transport. J. Atmos. Sci., **66**, 1465-1487, doi:10.1175/2008JAS2635.1.

Neggers, R.A.J., 2009. A dual mass flux framework for boundary layer convection. Part II: Clouds. J. Atmos. Sci., **66**, 1489-1506, doi:10.1175/2008JAS2636.1.

Schaap, M., R.M.A. Timmermans, M. Roemer, G.A.C. Boersen, P.J.H. Builtjes, F.J. Sauter, G.J.M. Velders & J.P. Beck, 2008. The LOTOS-EUROS model: description, validation and latest developments, Int. J. Environment and Pollution, **32** (2), 270-290.

Siebesma, A.P., P.M.M. Soares & J. Teixeira, 2007. A Combined Eddy-Diffusivity Mass-Flux Approach for the Convective Boundary Layer. J. Atmos. Sci., **64**, 1230-1248, doi:10.1175/JAS3888.1.

Sterl, A., H. van den Brink, H. de Vries, R. Haarsma & E. van Meijgaard, 2009. An ensemble study of extreme North Sea storm surges in a changing climate. Ocean Science **5**, 369-378.

Uppala, S.M., & 45 co-authors, 2005. The ERA-40 re-analysis. Q. J. R. Meteorol. Soc., **131**, 2961–3012. doi:10.1256/qj.04.176.

Wipfler, E.L., K. Metselaar, J.C. van Dam, R.A. Feddes, E. van Meijgaard, L.H. van Ulft, B. van den Hurk, S.J. Zwart & W.G.M. Bastiaanssen, 2011. Seasonal evaluation of the land surface scheme HTESSEL against remote sensing derived energy fluxes of the Transdanubian region in Hungary, Hydrol. Earth Syst. Sci., **15**, 1257-1271. doi:10.5194/hess-15-1257-2011.

The scenario-approach in the Netherlands

Scenario-thinking

Scenarios are often used when uncertainties are too large to capture comprehensively and when it is difficult to attach probabilities to the various projections for the future. This is e.g. the case for climate change, but also for demographic and economic developments.

In climate change studies two contrasting approaches can be identified:

a. Top down approach (a sequence of uncertainty assessments ranging from the global climate signal to local climate impact);
b. Bottom up approach (vulnerability analysis, tipping point analysis).

In the first approach climate scenarios are used from the start, in the second approach climate scenarios may be used after a vulnerability analysis has been performed to estimate when climate change becomes critical.

The CcSP program has been strongly driven by the existing practice of assessing the effects of future climate change on various sectors in the Netherlands. This practice is based on the use of a discrete number of future scenarios, for climate, demographic or economic developments. It is often much more a top down than a bottom up approach.

Discussions between (climate) scientists and information users reflect several of the shortcomings of a discrete set of scenarios: questions are raised frequently about the likelihood of several scenarios, and the desire to make available new scenarios for conditions not covered by KNMI'06. During the CcSP program also discussions emerged concerning the usefulness and limitations of climate scenarios derived with the top-down approach. Alternative (bottom-up) approaches are increasingly explored, including probabilistic projections (encompass a wide range of future conditions), tipping

point analyses (when do changes occur that have a strong effect on society?) and vulnerability analyses that underlie the "hotspot" approach in the Knowledge for Climate program.

The development and applicability of KNMI '06 scenarios

With the development of KNMI'06 scenarios (partially based on Regional Climate Model (RCM) simulations performed within CS6) and the user consultation and applied tailoring of climate information (in CS7), we have attempted to bridge a gap between the two approaches mentioned before. The first approach fails when the scenarios do not sufficiently highlight conditions to which a specific application is sensitive and vulnerable. In that case tailoring may be a solution. The second approach fails when stakeholders can not diagnose conditions to which the specific application is sensitive/vulnerable. In that case climate scenarios might be used in the search for these thresholds, although in a pure bottom-up approach scenarios are typically used after the vulnerability analysis.

With KNMI'06 we have provided the community with a limited number of scenarios that are mutually sufficiently diverse to allow a wide range of users to assess consequences of climate change without claiming that these scenarios span all sources of uncertainty. We treat these discrete scenarios as "stories" of possible future conditions, and generate detailed tailored information to allow users to translate these stories for their own practice.

Next generation climate scenarios

Further development of the methods to construct scenarios is currently intensely discussed within the context of the next generation of KNMI climate change scenarios, KNMInext. Higher levels of sophistication of tailored climate information will be made available through high resolution "Future weather" simulations, carefully selected to be consistent with a given set of scenario assumptions. A scientific paper by Hazeleger et al[1] is in preparation.

1 W. Hazeleger, B. van den Hurk, E. Min, A. Petersen, D. Stainforth, E. Vasileiadou; Tales of future weather; to be submitted to Nature Climate Change

Climate changes Spatial Planning

Climate change is one of the major environmental issues of this century. The Netherlands are expected to face climate change impacts on all land- and water related sectors. Therefore water management and spatial planning have to take climate change into account. The research programme 'Climate changes Spatial Planning', that ran from 2004 to 2011, aimed to create applied knowledge to support society to take the right decisions and measures to reduce the adverse impacts of climate change. It focused on enhancing joint learning between scientists and practitioners in the fields of spatial planning, nature, agriculture, and water- and flood risk management. Under the programme five themes were developed: climate scenarios; mitigation; adaptation; integration and communication. Of all scientific research projects synthesis reports were produced. This report is part of the Climate scenarios series.

Climate scenarios

The projects in this field are designed to obtain high quality climate information and scenarios relevant for the Netherlands. The projects both focus on an improved monitoring and modelling of regional climate variability, and at the construction of tailored climate change scenarios suitable for exploring spatial adaptation options, such as flood retention areas or coastal defense. In all fields special attention is devoted to extreme climate conditions. The climate scenarios are designed and developed jointly with a number of key stakeholders.

Programme Office Climate changes Spatial Planning

P.O. Box 1072
3430 BB Nieuwegein
The Netherlands
T +31 30 6069 780

c/o Alterra, Wageningen UR
P.O. Box 47
6700 AA Wageningen
The Netherlands
T +31 317 48 6540
info@klimaatvoorruimte.nl

www.climatechangesspatialplanning.nl